#9

N 57 50818

NATIONAL ADVISORY COMMITTEE FOR AERONAUTICS

REPORT No. 818

AN EXPERIMENTAL INVESTIGATION OF RECTANGULAR EXHAUST-GAS EJECTORS APPLICABLE FOR ENGINE COOLING

By EUGENE J. MANGANIELLO and DONALD BOGATSKY

THIS DOCUMENT ON LOAN FROM THE FILES OF

NATIONAL ADVISORY COMMITTEE FOR AERONAUTICS
LANGLEY MEMORIAL AERONAUTICAL LABORATORY
LANGLEY FIELD, HAMPTON, VIRGINIA

RETURN TO THE ABOVE ADDRESS.

REQUESTS FOR PUBLICATIONS SHOULD BE ADDRESSED AS FOLLOWS:

NATIONAL ADVISORY COMMITTEE FOR AERONAUTICS
1724 F STREET, N.W.,
WASHINGTON 25, D.C.

1945

For sale by the Superintendent of Documents, U. S. Government Printing Office, Washington 25, D. C. - - - - Price 20 cents

AERONAUTIC SYMBOLS

1. FUNDAMENTAL AND DERIVED UNITS

	Symbol	Metric		English	
		Unit	Abbreviation	Unit	Abbreviation
Length	l	meter	m	foot (or mile)	ft (or mi)
Time	t	second	s	second (or hour)	sec (or hr)
Force	F	weight of 1 kilogram	kg	weight of 1 pound	lb
Power	P	horsepower (metric)		horsepower	hp
Speed	V	kilometers per hour	kph	miles per hour	mph
		meters per second	mps	feet per second	fps

2. GENERAL SYMBOLS

W Weight$=mg$

g Standard acceleration of gravity$=9.80665$ m/s^2 or 32.1740 ft/sec^2

m Mass$=\frac{W}{g}$

I Moment of inertia$=mk^2$. (Indicate axis of radius of gyration k by proper subscript.)

μ Coefficient of viscosity

ν Kinematic viscosity

ρ Density (mass per unit volume)

Standard density of dry air, 0.12497 kg-m^{-4}-s^2 at 15° C and 760 mm; or 0.002378 lb-ft^{-4} sec^2

Specific weight of "standard" air, 1.2255 kg/m^3 or 0.07651 lb/cu ft

3. AERODYNAMIC SYMBOLS

S Area

S_w Area of wing

G Gap

b Span

c Chord

A Aspect ratio, $\frac{b^2}{S}$

V True air speed

q Dynamic pressure, $\frac{1}{2}\rho V^2$

L Lift, absolute coefficient $C_L=\frac{L}{qS}$

D Drag, absolute coefficient $C_D=\frac{D}{qS}$

D_0 Profile drag, absolute coefficient $C_{D_0}=\frac{D_0}{qS}$

D_i Induced drag, absolute coefficient $C_{D_i}=\frac{D_i}{qS}$

D_p Parasite drag, absolute coefficient $C_{D_p}=\frac{D_p}{qS}$

C Cross-wind force, absolute coefficient $C_C=\frac{C}{qS}$

i_w Angle of setting of wings (relative to thrust line)

i_t Angle of stabilizer setting (relative to thrust line)

Q Resultant moment

Ω Resultant angular velocity

R Reynolds number, $\rho\frac{Vl}{\mu}$ where l is a linear dimension (e.g., for an airfoil of 1.0 ft chord, 100 mph, standard pressure at 15° C, the corresponding Reynolds number is 935,400; or for an airfoil of 1.0 m chord, 100 mps, the corresponding Reynolds number is 6,865,000)

α Angle of attack

ϵ Angle of downwash

α_0 Angle of attack, infinite aspect ratio

α_i Angle of attack, induced

α_a Angle of attack, absolute (measured from zero-lift position)

γ Flight-path angle

REPORT No. 818

AN EXPERIMENTAL INVESTIGATION OF RECTANGULAR EXHAUST-GAS EJECTORS APPLICABLE FOR ENGINE COOLING

By EUGENE J. MANGANIELLO and DONALD BOGATSKY

Aircraft Engine Research Laboratory
Cleveland, Ohio

National Advisory Committee for Aeronautics

Headquarters, 1500 New Hampshire Avenue NW., Washington 25, D. C.

Created by act of Congress approved March 3, 1915, for the supervision and direction of the scientific study of the problems of flight (U. S. Code, title 49, sec. 241). Its membership was increased to 15 by act approved March 2, 1929. The members are appointed by the President, and serve as such without compensation.

JEROME C. HUNSAKER, Sc. D., Cambridge, Mass., *Chairman*

LYMAN J. BRIGGS, Ph. D., *Vice Chairman*, Director, National Bureau of Standards.

CHARLES G. ABBOT, Sc. D., *Vice Chairman, Executive Committee*, Secretary, Smithsonian Institution.

HENRY H. ARNOLD, General, United States Army, Commanding General, Army Air Forces, War Department.

WILLIAM A. M. BURDEN, Assistant Secretary of Commerce for Aeronautics.

VANNEVAR BUSH, Sc. D., Director, Office of Scientific Research and Development, Washington, D. C.

WILLIAM F. DURAND, Ph. D. Stanford University, California.

OLIVER P. ECHOLS, Major General, United States Army, Chief of Matériel, Maintenance, and Distribution, Army Air Forces, War Department.

AUBREY W. FITCH, Vice Admiral, United States Navy, Deputy Chief of Naval Operations (Air), Navy Department.

WILLIAM LITTLEWOOD, M. E., Jackson Heights, Long Island, N. Y.

FRANCIS W. REICHELDERFER, Sc. D., Chief, United States Weather Bureau.

LAWRENCE B. RICHARDSON, Rear Admiral, United States Navy, Assistant Chief, Bureau of Aeronautics. Navy Department.

EDWARD WARNER, Sc. D., Civil Aeronautics Board, Washington, D. C.

ORVILLE WRIGHT, Sc. D., Dayton, Ohio.

THEODORE P. WRIGHT, Sc. D., Administrator of Civil Aeronautics, Department of Commerce.

GEORGE W. LEWIS, Sc. D., *Director of Aeronautical Research*

JOHN F. VICTORY, LL. M., Secretary

HENRY J. E. REID, Sc. D., Engineer-in-Charge, Langley Memorial Aeronautical Laboratory, Langley Field, Va.

SMITH J. DEFRANCE, B. S., Engineer-in-Charge, Ames Aeronautical Laboratory, Moffett Field, Calif.

EDWARD R. SHARP, LL. B., Manager, Aircraft Engine Research Laboratory, Cleveland Airport, Cleveland, Ohio

CARLTON KEMPER, B. S., Executive Engineer, Aircraft Engine Research Laboratory, Cleveland Airport, Cleveland, Ohio

TECHNICAL COMMITTEES

AERODYNAMICS

POWER PLANTS FOR AIRCRAFT

AIRCRAFT CONSTRUCTION

OPERATING PROBLEMS

MATERIALS RESEARCH COORDINATION

Coordination of Research Needs of Military and Civil Aviation

Preparation of Research Programs

Allocation of Problems

Prevention of Duplication

LANGLEY MEMORIAL AERONAUTICAL LABORATORY
Langley Field, Va.

AMES AERONAUTICAL LABORATORY
Moffett Field, Calif.

AIRCRAFT ENGINE RESEARCH LABORATORY, Cleveland Airport, Cleveland, Ohio

Conduct, under unified control, for all agencies, of scientific research on the fundamental problems of flight

OFFICE OF AERONAUTICAL INTELLIGENCE, Washington, D. C.

Collection, classification, compilation, and dissemination of scientific and technical information on aeronautics

REPORT No. 818

AN EXPERIMENTAL INVESTIGATION OF RECTANGULAR EXHAUST-GAS EJECTORS APPLICABLE FOR ENGINE COOLING

By Eugene J. Manganiello and Donald Bogatsky

SUMMARY

An experimental investigation of rectangular exhaust-gas ejector pumps was conducted to provide data that would serve as a guide to the design of ejector applications for aircraft engines with marginal cooling. The pumping characteristics of rectangular ejectors actuated by the exhaust of a single-cylinder aircraft engine were determined for a range of ejector mixing-section area from 20 to 50 square inches, over-all length from 12 to 42 inches, aspect ratio from 1 to 5, diffusing exit area from 20 to 81 square inches, and exhaust-nozzle aspect ratio from 1 to 42. A few tests were conducted with a multi-stage ejector, a divided ejector, and an ejector incorporating bends along its length.

With a decrease in the quantity of air pumped and an increase in the length of ejector, the ejector pressure rise increases to optimum values. Optimum values of ejector area were found to depend upon mass-flow ratio of air to exhaust gas for given engine operating conditions. Diffuser-exit sections considerably improved the performance of the ejectors. An arrangement of a straight mixing section with a diffusing exit and a flattened exhaust nozzle provided the most favorable ejector performance. An ejector composed of a straight mixing section of 24-inch length and 25-square-inch area with a diffusing exit of 12-inch length and 1.87 exit-area—entrance-area ratio provided a pressure rise of 6 inches of water for a mass flow of air representative of cooling requirements (six times the mass flow of exhaust gas) for the engine when operated at a cruise power of 85 indicated horsepower.

A simplified analysis, which considers the effect of pertinent ejector variables and indicates the performance in terms of known engine quantities, was made. The agreement between theory and experiment was fair over the range of ejector configurations tested, except that a serious discrepancy existed in that the optimum ejector areas prescribed by theory were smaller and the values of peak pressure rise predicted at the small optimum areas were higher than indicated by the tests.

INTRODUCTION

The cooling problem has been one of the main obstacles to the attainment of high power outputs with modern air-cooled aircraft engines. Adequate cooling on the ground, in climb, and in long-range cruise has been difficult to obtain in most submerged and pusher-type installations, and in some high-performance tractor installations. The possibility of the use of ejector pumps actuated by the engine exhaust has been suggested as a means of providing the additional cooling-air pressure drop required in installations with marginal cooling.

Some experimental investigations of the ejector principle have been made in connection with aircraft problems. References 1 and 2 present results of ejector tests with regard to jet-thrust augmentation. The tests were conducted, for the most part, with small-scale models actuated by compressed air under steady-flow conditions. An investigation of the design and operating conditions of small-scale compressed-air ejectors, the results of which are pertinent to their pumping as well as to their thrust-augmentation characteristics, has been conducted at the United Aircraft Corporation. In reference 3 results are presented of a preliminary investigation made to determine the suitability of ejectors actuated by the exhaust of a radial aircraft engine for providing engine cooling air at the ground condition. The pressure drops realized with some of the ejector combinations investigated in reference 3 were of significant magnitude for cooling. Tests made at the Northrop Aircraft, Inc. of a number of exhaust-ejector systems for cooling aircraft engines showed that appreciable improvement in cooling could be obtained by the use of ejectors.

In view of the results presented in references 1 to 3 and of the general interest in ejector cooling augmentation, the present investigation was conducted at Langley Field, Va., in the fall of 1942 to obtain additional quantitative information on the performance of exhaust-gas ejector pumps and to provide design data for the application of ejectors to aircraft-engine installations. The publication of the results was delayed by the transfer of the staff and equipment to Cleveland, Ohio.

The experimental work was performed on ejectors of rectangular cross section actuated by the exhaust from a single-cylinder aircraft engine. The pumping characteristics of ejectors of various area were determined for a range of length, aspect ratio, diffusing exit, and shape of exhaust nozzle. Ejectors of rectangular cross section were tested because it was felt that this approximate shape would readily lend itself to installation on engine cowls of conventional configuration. Engine power was limited to about the cruise value (70 percent rated). A simplified theoretical analysis was made that indicates ejector performance in terms of known engine and exhaust-gas quantities.

1

ANALYSIS

An ejector is a device in which the kinetic energy of one fluid is used to pump another fluid from a region of low pressure to a region of high pressure.

In the present application, consideration is given to the use of the high-velocity exhaust-gas jets that issue from the individual exhaust stacks of the cylinders of an aircraft engine for pumping cooling air from the rear of the engine to the atmosphere. The effect of ejector action, then, is to reduce the static pressure behind the engine and thus to increase the pressure drop available for cooling. Ejector action is affected by the transfer of momentum between the high-velocity exhaust-gas jet and the low-velocity air in the mixing section.

An ejector may be designed for constant pressure throughout the mixing section, in which case it has little value as a pump; on the other hand, a constant-area mixing section permits operation with a pressure rise and is therefore pertinent to the present application. The addition of a diffusing exit to the constant-area mixing section results in a further pressure rise owing to the conversion of velocity head.

A theoretical equation for the pressure rise across the ejector is derived in the appendix and incorporates the assumptions that follow.

The exhaust process in an engine is an intermittent one in which the mass-flow rate, the velocity, and therefore the momentum of the exhaust gas vary cyclically. Consequently, the inflowing air and the outflowing mixture in the ejector actuated by the exhaust gas will be of a pulsating nature. The effect of the pulsating exhaust gas is taken into account by the use of a mean effective exhaust-gas velocity $\overline{V}_e$, which is introduced in reference 4 as the equivalent velocity that, when multiplied by the steady-flow average mass-flow rate of exhaust gas, would produce the average momentum obtained by thrust measurements. Unfortunately, a similar treatment is not readily applicable to the air that enters and the mixture that leaves the ejector. In view of the complicated nature of the pulsating air and the mixture flow and their dependence upon mass-flow rate, ejector dimensions, and engine operating conditions, steady-flow values are assumed. Inasmuch as the pulsations in the air flow are damped relative to those existing in the exhaust-gas flow, the deviations incurred by the foregoing assumption should not be serious.

The assumptions of complete mixing and absence of wall friction are made. The pressure rise obtained with an ejector is then expected to be somewhat less than that predicted by theory. In an actual ejector, both the degree of completeness of mixing and the friction losses increase with increase of ejector length. The pressure rise, however, is so affected by these opposing factors as to produce an optimum length.

The additional assumption of a uniform velocity distribution across the ejector area is postulated. Actually, the air entering the mixing section is accelerated by contact with the high-velocity exhaust-gas jet with the result that the ejector cross-sectional area surrounding the jet is more effective in conducting the mass flow of gases than the area adjacent to the walls. The effective flow area may be further decreased by the increased flow resistance of the corner regions of the rectangular ejector. Hence, the observed pressure rises will not be compatible with the theoretical pressure rises for an ejector of the same area. A more favorable comparison is possible with theoretical pressure rises for some arbitrarily reduced area.

The expression for the pressure rise across the ejector subject to the foregoing assumptions, as derived in the appendix, is given by equation (19),

$$\Delta p=\frac{M_e\overline{V}_e}{A_2}+\left(\frac{M_e}{A_2}\right)^2\frac{1}{\rho_a}\frac{M_a}{M_e}\left[\frac{\alpha}{2}\frac{M_a}{M_e}+\left(\frac{M_e}{M_a}+1\right)\left(\frac{M_a}{M_e}+\frac{R_e}{R_a}\right)\left(\frac{\frac{M_a}{M_e}+\frac{c_{p,e}}{c_{p,a}}\frac{T_e}{T_a}}{\frac{M_a}{M_e}+\frac{c_{p,e}}{c_{p,a}}}\right)\left(\frac{\beta}{2}-1\right)\right] \tag{19}$$

The symbols used in this equation are defined in the appendix.

This equation will be considered as the general expression for evaluating the performance of the tested ejectors both with and without a diffuser exit; for nondiffusing ejectors, the diffuser factor β is equal to 0.

If the difference in specific heat and gas constant of air and exhaust gas is neglected and the area of the exhaust-gas jet is small (that is, the factor α accounting for the reduction of the ejector-entrance area due to the presence of the exhaust-gas jet is unity) equation (19) may be simplified to

$$\Delta p=\frac{M_eV_e}{A_2}+\left(\frac{M_e}{A_2}\right)^2\frac{1}{\rho_a}\frac{M_a}{M_e}\left[\frac{1}{2}\frac{M_a}{M_e}+\left(\frac{M_a}{M_e}+1\right)\left(1+\frac{M_e}{M_a}\frac{T_e}{T_a}\right)\left(\frac{\beta}{2}-1\right)\right] \tag{20}$$

which may be expressed as

$$\Delta p=\frac{M_e\overline{V}_e}{A_2}+\left(\frac{M_e}{A_2}\right)^2\frac{1}{\rho_a}f\left(\frac{M_a}{M_e},\frac{T_e}{T_a}\right)$$

In the range of ejector operation of practical interest in the present application, the use of equation (20) introduces slight deviations from the pressure rises predicted by equation (19).

If a nondiffusing or straight ejector is first considered, inspection of general equation (19) indicates that the pressure rise is a function of several variables; namely, area of ejector, mass-flow rate and mean effective velocity of exhaust-gas jet, mass-flow ratio of air to exhaust gas M_a/M_e, density of air, and temperature ratio of exhaust gas to air. In the present application, all of the variables except ejector area are specified or are known from the desired engine operating conditions. The mass-flow rate of exhaust gas is specified by engine power and the mass-flow rate of cooling air is known from the cooling characteristics of the engine. (Representative values of M_a/M_e lie between 6 and 9.) The temperature and the density of the air are determined by the ejector-inlet conditions. A representative value of 1500° F may be used for the temperature of the exhaust gas inasmuch as large variations from this value have inappreciable effect upon the results. The velocity of the exhaust-gas jet is determined by the engine operating conditions and by the area of the exhaust-gas nozzle. For maximum ejector performance, small nozzle areas are indicated; the minimum nozzle area is, however, limited by considerations of engine-power loss. Reference 4 provides information for determining the minimum permissible nozzle area and also the mean effective exhaust-gas velocity from the engine operating conditions. The mean effective velocity is the value obtained by dividing the average exhaust-gas thrust, as measured with a target, by the average mass-flow rate of exhaust gas; hence, it is directly applicable to the ejector equation.

When the values of the foregoing variables are inserted in the general equation, the pressure rise is reduced to a function of the area of the form

$$\Delta p = \frac{C_1}{A} - \frac{C_2}{A^2}$$

where C_1 and C_2 are constants.

For a diffuser ejector, this equation is modified simply by a reduction in the absolute value of the negative term to an extent determined by the expansion ratio of the diffuser.

The theoretical curves were obtained from equation (19). In the calculation of the theoretical curves for comparison with the test results, the following values were used:

Mass-flow rate of exhaust gas, pounds per minute	8
Mean effective exhaust-gas velocity (obtained from reference 4 for the 2.6 sq in. nozzle area and the atmospheric exhaust used), feet per second	1625
Density of air (atmospheric), slugs per cubic foot	0. 00232
Temperature of exhaust gas, °F	1500
Temperature of air (average value maintained throughout tests), °F	75
Specific heat of exhaust gas, Btu per pound per °F	0. 29
Specific heat of air, Btu per pound per °F	0. 24
Gas constant of exhaust gas, foot-pounds per pound per °F	56. 4
Gas constant of air, foot-pounds per pound per °F	53. 3
Diffuser-loss coefficient	0. 15

The performance of ejectors of various area was then calculated for a range of M_a/M_e from 3 to 16.

APPARATUS AND METHODS

The test-engine setup and the auxiliary equipment used for this investigation are shown in figure 1 and the arrangement of the apparatus is further indicated diagrammatically in figure 2. The single-cylinder test engine was an 1820–G

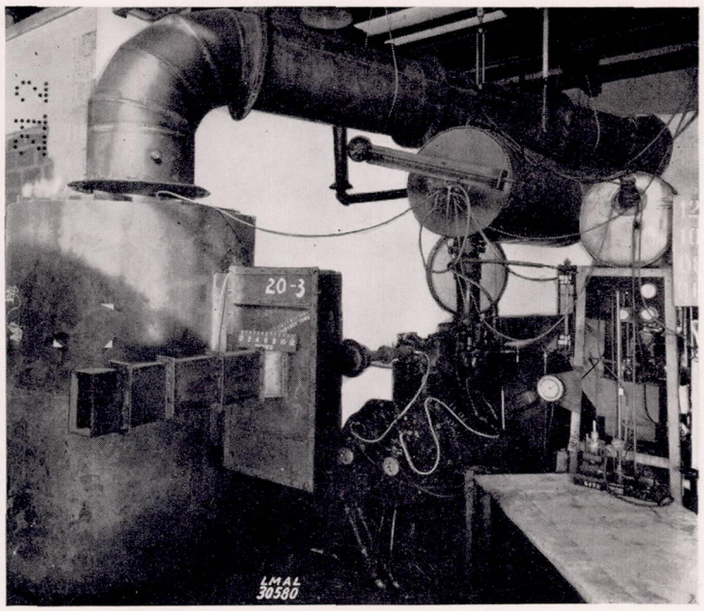


FIGURE 1.—Ejector setup.

engine modified to operate with only one cylinder. The air-cooled cylinder was enclosed in a sheet-metal jacket open at the front and connected at the rear to a motor-driven centrifugal blower that provided the necessary engine cooling air. An electric dynamometer was used to load the engine and to measure the engine torque. Engine speed was measured by an electrically operated revolution counter and a stop watch.

The charge-air weight flow of the engine was measured by a thin-plate orifice installed according to A.S.M.E. standards. A surge tank was provided between the engine and the orifice to damp out pulsations. Upstream and differential pressures at the orifice were measured with a mercury and a water manometer, respectively. The fuel-flow measurements were obtained with a calibrated rotameter. The weight flow of the air pumped by ejector action was measured by means of a large intake-orifice pipe (reference 5); an alcohol micromanometer was used to indicate the small pressure drops across the orifice plate. The downstream end of the orifice pipe was connected to a cylindrical surge tank with a volume of approximately 90 cubic feet to which was attached an extension chamber with provision for mounting the various ejectors. The static pressure in the surge tank and in the extension chamber was controlled by a butterfly valve installed between the orifice pipe and the surge tank and was measured with a water manometer.

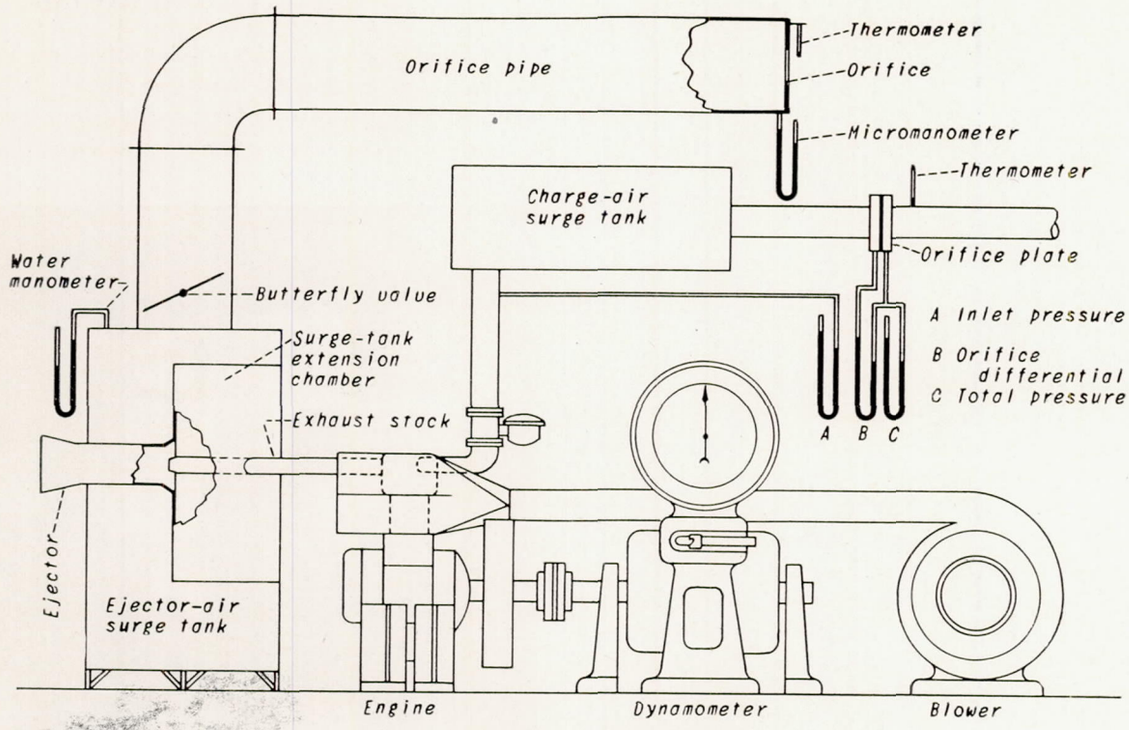


FIGURE 2.—Diagrammatic layout of equipment.

The engine exhaust stack, consisting of a $2\frac{5}{16}$-inch-inside-diameter pipe, was led through a flexible connection into the extension chamber and was provided with a flanged end to permit the attachment of nozzles of various shapes. The nozzle-exit area was 2.6 square inches, calculated from reference 4, for zero power loss at an engine speed of 2100 rpm, a manifold pressure of 35 inches of mercury, and an exhaust pressure equal to that at sea level. The nozzle exits were centrally located in the convergent entrance sections of the ejector; their axial position was varied by spacers.

Ejectors of rectangular cross section were chosen for the tests despite the inherently greater strength and stability of the circular form. This choice was prompted by consideration of the aerodynamic aspects of an actual ejector installation on a conventional cowl where approximately rectangular shape would permit more efficient utilization of available space.

Each ejector was composed of a convergent entrance section and a constant-area mixing section; the addition of a diffusing exit section to the mixing section formed a diffuser ejector. The convergence of the entrance section and the divergence of the exit section were confined only to the vertical plane; this procedure was dictated by consideration of space limitations in an actual installation.

For a given ejector area, the entrance sections were constructed with a ratio of entrance area to ejector area of 3.06. The lengths of these entrance sections were equal to the lengths of a 60° right conical section of the same entrance and exit areas. It was felt that this configuration would permit the most economical space utilization without sacrifice in ejector performance. Mounting plates were welded to the entrance sections to provide attachment to the surge-tank extension chamber.

The diffusing exit sections were built with an included angle of 12°. Reference 6 indicates that a negligible increase in shock loss above minimum value is incurred with this expansion angle for rectangular diffusers with single-plane divergence.

TABLE I.—STRAIGHT AND DIFFUSER EXHAUST-GAS EJECTORS INVESTIGATED

Ejector				Exhaust nozzle		
Straight-section area (sq in.)	Aspect ratio [a]	Diffuser-area ratio [b]	Designation [c]	Aspect ratio [a]	Exit location [d] (in.)	Figure
20	3	----------	18S	15.8	1	4 (a)
			24S	15.8	1	
			30S	15.8	1	
			36S	15.8	1	
25	3	----------	12S	12.0	0	4 (b)
			18S	12.0	0	
			24S	12.0	0	
			30S	12.0	0	
30	3	----------	18S	15.8	0	4 (c)
			24S	15.8	0	
			30S	15.8	0	
			36S	15.8	0	
50	3	----------	18S	41.7	0	4 (d)
			24S	41.7	0	
20	3	1.49	18S+6D	15.8	1	7 (a)
			24S+6D	15.8	1	
			30S+6D	15.8	1	
25	3	1.44	6S+6D	12.0	0	7 (b)
			12S+6D	12.0	0	
			18S+6D	12.0	0	
			24S+6D	12.0	1	
			30S+6D	12.0	1	
30	3	1.40	24S+6D	15.8	0	7 (c)
50	3	1.31	18S+6D	41.7	0	7 (d)
20	3	1.98	12S+12D	15.8	1	8 (a)
			18S+12D	15.8	1	
25	3	1.87	6S+12D	12.0	0	8 (b)
			12S+12D	12.0	0	
			18S+12D	12.0	1	
			24S+12D	12.0	1	
30	3	1.80	18S+12D	15.8	0	8 (c)
			24S+12D	15.8	0	
			30S+12D	15.8	0	
50	3	1.62	12S+12D	41.7	0	8 (d)
25	3	2.75	24D	12.0	0	10
		2.31	6S+18D	12.0	0	
25	1	----------	24S	1.0	0	15
30	5	----------	36S	15.8	0	
		2.03	18S+12D	15.8	0	
25	1	1.76	6S+18D	7.0	0	18 (a)
		1.76	6S+18D	1.0	0	
30	3	1.80	18S+12D	12.0	0	
	5	1.51	24S+6D	41.7	0	
	5	1.51	24S+6D	15.8	0	
30	3	1.80	18S+12D	15.8	1	18 (b)

[a] Ratio of larger to smaller dimension of rectangular straight section and of nozzle exit. (Nozzle-exit area, 2.6 sq in.)
[b] Ratio of exit area to entrance area of diffuser.
[c] S, straight section; D, diffuser. (Numbers refer to length in in.) Example: 24S+6D implies a 24-in. straight section+a 6-in. diffuser.
[d] Distance, in in. axially back from midplane of convergent-entrance section.

Table I presents a summary of the ejector configurations tested and figure 3 indicates the details and terminology of a representative ejector. The configurations are divided into two general groups: first, straight ejectors consisting of converging entrance sections and constant-area mixing sections, and second, diffuser ejectors consisting of diverging exit sections appended to the straight ejectors. Straight-section areas of 20, 25, 30, and 50 square inches were investigated over a range of over-all length from 6 to 36 inches for both groups. Diffusing exits were tested in lengths of 6, 12, and, for a few cases, 18 inches. In regard to the maximum length tested, no attempt was made to cover the range of length required to obtain maximum ejector performance for all areas investigated. Instead, the lengths were limited to values that were considered compatible with available space on conventional aircraft power-plant installations. An ejector aspect ratio of 3 (the ratio of the larger to the smaller dimension of the rectangular straight section) was arbitrarily chosen for most of the tests from a rough consideration of how the ejectors might be installed on the periphery of the nacelle of a radial engine. A few tests, however, were conducted with ejector aspect ratios of 1 and 5 for comparative purposes. The exhaust-nozzle aspect ratio was varied with each ejector area in an effort to obtain improved performance; the total range covered extended from a square nozzle to a wide flat nozzle with an aspect ratio of about 40. In a number of tests, the location of the nozzle exit was varied from a central axial position in the ejector-entrance section to a position farther back.

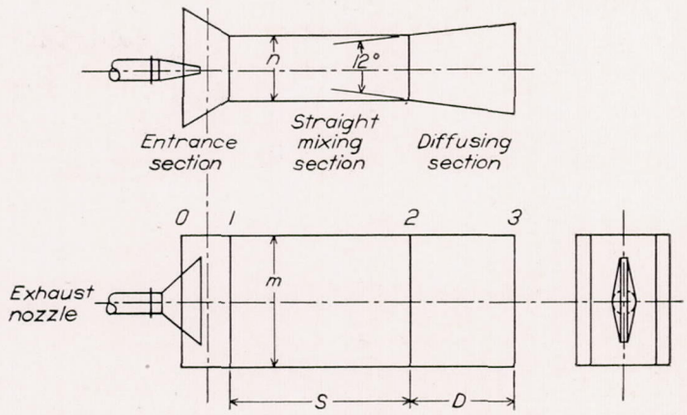
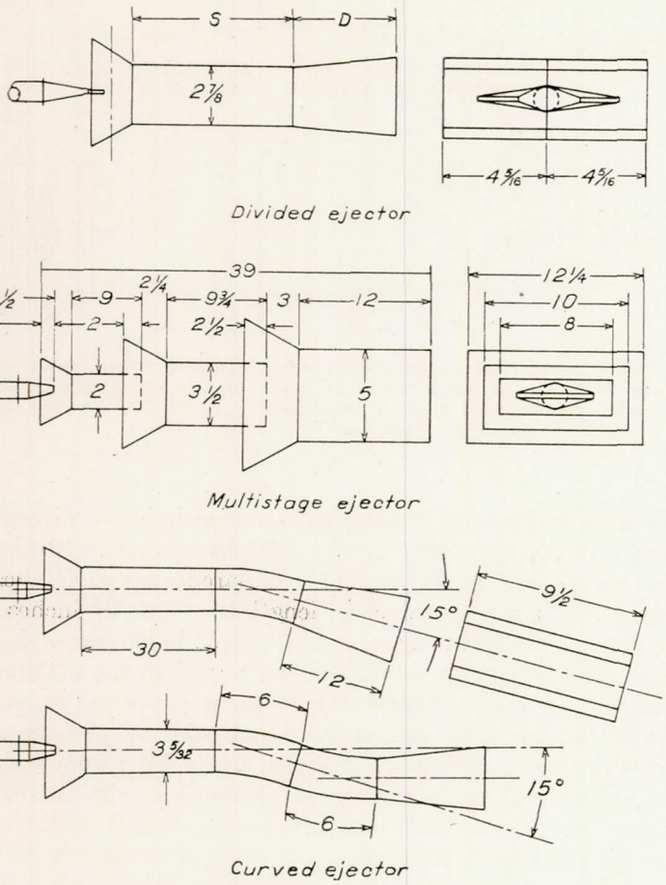


FIGURE 3.—Ejector details and terminology. Straight mixing-section area, square inches; aspect ratio of straight mixing section m/n; length of straight mixing section S, inches; length of diffusing section D, inches. (For example, an ejector with a straight section of 24 in. and a diffusing section of 12 in. would be designated 24S+12D.)

TABLE II.—SPECIAL EXHAUST-GAS EJECTORS INVESTIGATED



Ejector					Exhaust nozzle		
Type	Straight-section area (sq in.)	Aspect ratio [a]	Diffuser-area ratio [b]	Designation [c]	Aspect ratio [a]	Exit location [d] (in.)	Figure
Divided	25	1.5	1.87	12S+12D	5.2	1	16
			1.87	12S+12D	5.2	0	
			-----	30S	5.2	0	
Three stage	16	4.0	-----	9S	12.0	0	17
	35	2.85	-----	9.75S			
	61	2.45	-----	12S			
Single bend	30	3.0	1.80	30S+6B+12D	15.8	0	14
Reverse bend	30	3.0	1.80	30S+6B+6B+12D	15.8	0	

[a] Ratio of larger to smaller dimension of rectangular straight section and of nozzle exit. (Nozzle-exit area, 2.6 sq in.)
[b] Ratio of exit area to entrance area of diffuser.
[c] S, straight section; D, diffuser; B, bend. (Numbers refer to length in in.)
[d] Distance, in in., axially back from midplane of convergent entrance section.

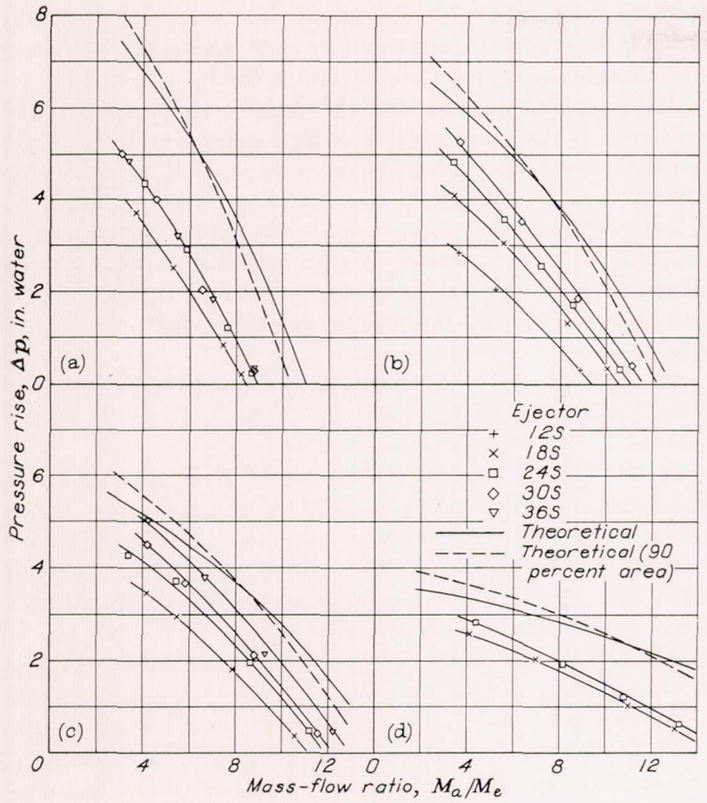
In addition to the foregoing simple ejectors, tests were conducted with several special arrangements shown in table II. The 25-square-inch ejector was divided into two equal ejectors by the installation of a dividing plate throughout its length. For this arrangement the exhaust stack was branched into two identical nozzles, each with an exit area of half that of an ordinary nozzle. These nozzles were centrally located in the divided ejector-entrance section. Tests were conducted to determine whether the increased length—hydraulic-diameter ratio for the same over-all length and total area would improve the performance. One multistage ejector, consisting of three straight ejectors in a series, was tested.

Inasmuch as application of ejectors to an aircraft installation might require some bends or curves along the ejector length, several tests were made with single- and reverse-curved lengths inserted in the mixing section of the 30-square-inch ejectors.

During the initial phase of the investigation, the ejector characteristics were determined over a range of engine powers. The limitations of the setup did not permit engine operation above atmospheric manifold pressure and above an engine speed of 2000 rpm, which gave a maximum engine power of 85 indicated horsepower. At a fuel-air ratio of 0.08, these operating conditions resulted in an exhaust-gas mass-flow rate of 8 pounds per minute. At an appreciably lower power output, the performance of the ejectors was of no practical interest; hence, most of the tests were conducted at the maximum obtainable engine power. For each ejector combination tested, the pressure rise across the ejector (that is, the difference in surge-tank and atmospheric pressures) was varied from the minimum to the maximum obtainable in four or five steps by means of the butterfly valve. The quantity of air pumped was measured at each condition.

DISCUSSION

Straight ejectors.—The performance of the straight or constant-area ejectors is shown in figure 4, where the rise in pressure across the ejector is plotted against M_a/M_e. Ejector details and terminology are shown in figure 3. Experimental results are presented for ejectors with an aspect ratio of 3, with areas of 20, 25, 30, and 50 square inches, and over a range of ejector length for an exhaust-nozzle area of 2.6 square inches and engine operating conditions of 85 indicated horsepower, engine speed of 2000 rpm, and fuel-air ratio of 0.08. The mass-flow rate of exhaust gas for these conditions was 8 pounds per minute. The exit aspect ratio of the exhaust nozzle used with the ejector of 50-square-inch area was about three times that of the nozzles used with the other ejectors. The wide nozzle was chosen in this case in order to distribute the exhaust jet across the ejector area and thus to provide mixing comparable with that obtained with the other ejectors. Theoretical curves obtained from equation (19) are included for comparison. Theoretical curves for 90 percent of the actual area gave the best all-round agreement with the experimental results for all the straight ejectors. For a given area, the pressure rise resulting from ejector action decreases as the quantity of air pumped is increased. An increase in area increases the range of mass-flow operation. The experimental curves are similar to the analytical curves and approach them in magnitude for the ejectors of longer length.



(a) Area, 20 square inches.
(b) Area, 25 square inches.
(c) Area, 30 square inches.
(d) Area, 50 square inches.

FIGURE 4.—Performance curves for straight ejectors actuated by exhaust of single-cylinder engine. Aspect ratio, 3; exhaust-gas mass-flow rate, 8 pounds per minute; exhaust-nozzle area, 2.6 square inches; fuel-air ratio, 0.08; indicated horsepower, 85. For further details see table I.

In figure 5 the results of figure 4 are cross-plotted against the length of ejector expressed in hydraulic diameters L/D_h for an M_a/M_e of 6. The optimum length was reached for the 20-square-inch ejector at an L/D_h of about 8 but the performance was not appreciably improved with an increase in length above an L/D_h of 6. The declining rate of increase of pressure rise with increase in length is explained by the opposing effects of increasing friction losses and more complete mixing benefits. The results for the ejectors of 25- and 30-square-inch area show that optimum lengths were not attained; the curves started to level off, however, at an L/D_h of about 6 or 7. Greater lengths than those tested would very likely have resulted in improved performance for ejectors of larger area; as previously explained, the maximum lengths used were limited by practical considerations of installations on aircraft.

A comparison of the performances of ejectors of various area in figure 4 indicates that the optimum area depends on M_a/M_e. With increasing M_a/M_e, maximum obtainable pressure rise is realized with the larger-area ejectors tested. Faired curves of pressure rise against ejector area are cross-plotted from figure 4 on figure 6 for values of M_a/M_e of 6 and 9, which are representative of the range of cooling-air requirement of modern aircraft engines. Only theoretical curves for 90 percent of the actual area are included for comparison; the full-area theoretical curves are omitted for clarity. The experimental and theoretical curves are similar in shape and exhibit fair agreement in magnitude at the large areas. Serious discrepancies, however, exist at the small

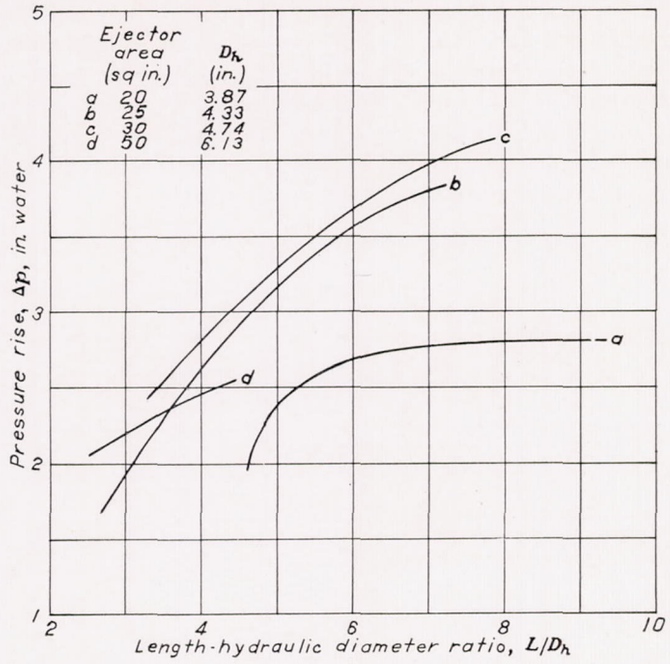


FIGURE 5.—Variation of pressure rise with length—hydraulic-diameter ratio for straight ejectors actuated by exhaust of single-cylinder engine. Aspect ratio, 3; exhaust-gas mass-flow rate, 8 pounds per minute; exhaust-nozzle area, 2.6 square inches; fuel-air ratio, 0.08; indicated horsepower, 85; mass-flow ratio, 6.

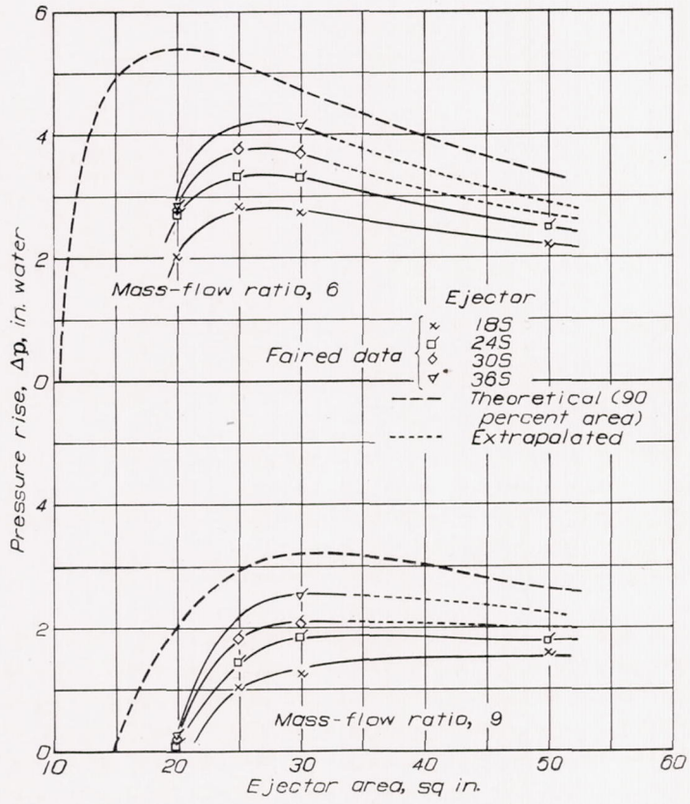
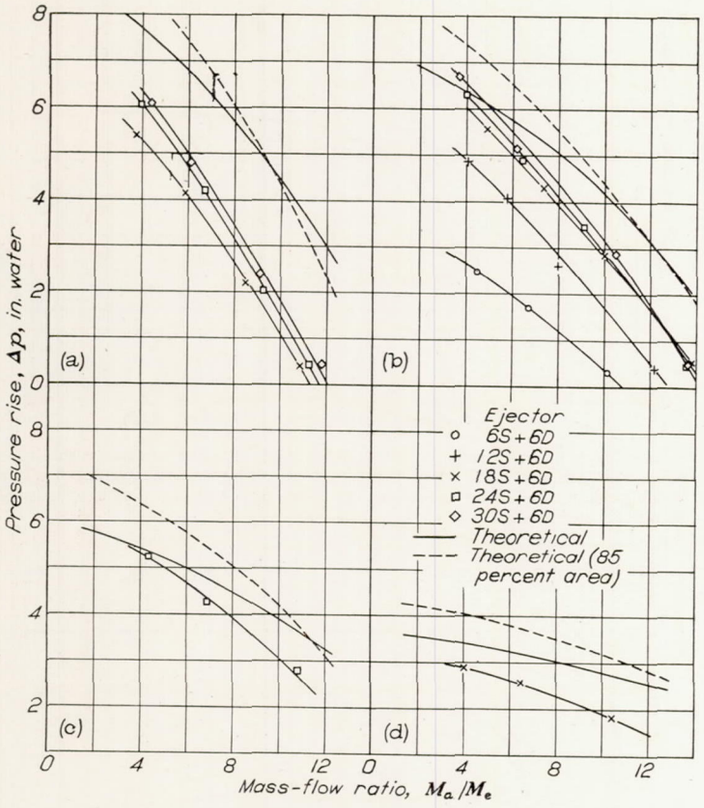


FIGURE 6.—Variation of pressure rise with ejector area for straight ejectors actuated by exhaust of single-cylinder engine. Aspect ratio, 3; exhaust-gas mass-flow rate, 8 pounds per minute; exhaust-nozzle area, 2.6 square inches; fuel-air ratio, 0.08; indicated horsepower, 85.

780395—48——2

areas; the theory predicts appreciably higher pressure rise and smaller optimum area than obtained by experiment. For example, at an M_a/M_e of 6, optimum area for the ejector of 30-inch length was observed at about 27 square inches with a pressure rise of 3.8 inches of water, whereas theory predicts the optimum area to be about 20 square inches with a pressure rise of 5.4 inches of water. This behavior is not without precedent; Flügel (reference 7) indicated that the minimum cross-sectional area required for steady-flow application has been found by experience to be from 30 to 50 percent greater than that prescribed by theory.

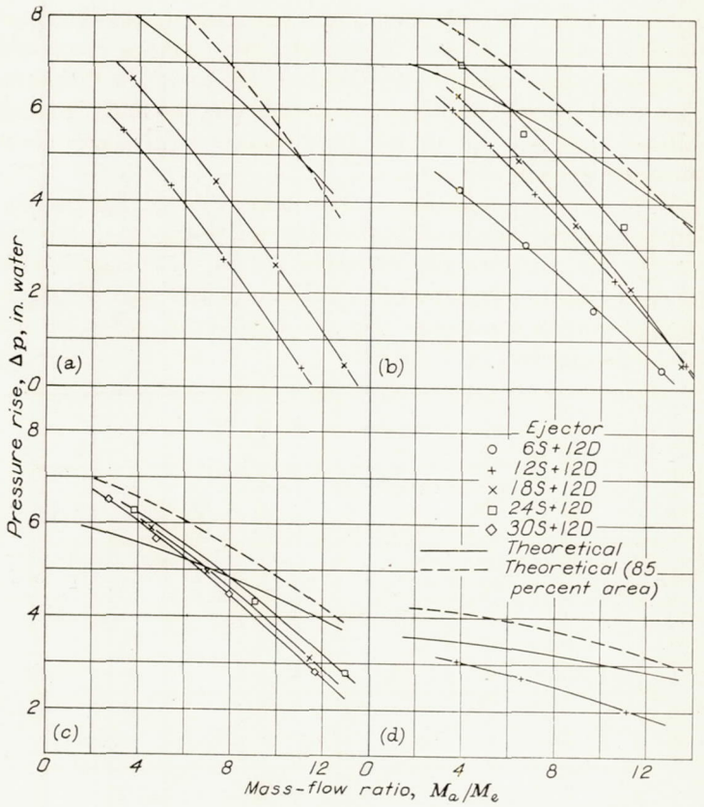


(a) Area, 20 square inches; diffuser-area ratio, 1.49.
(b) Area, 25 square inches; diffuser-area ratio, 1.44.
(c) Area, 30 square inches; diffuser-area ratio, 1.40.
(d) Area, 50 square inches; diffuser-area ratio, 1.31.

FIGURE 7.—Performance curves for 6-inch diffuser ejectors actuated by exhaust of single-cylinder engine. Aspect ratio, 3; exhaust-gas mass-flow rate, 8 pounds per minute; exhaust-nozzle area, 2.6 square inches; fuel-air ratio, 0.08; indicated horsepower, 85. For further details see table I.

Diffuser ejectors.—The performances of ejectors with 6- and 12-inch diffusing exits are shown in figures 7 and 8, respectively. The results are plotted in the same manner and for the same engine conditions as for the straight ejectors. The theoretical and experimental performance is seen to be essentially of the same nature as that noted for the straight ejectors. The values of pressure rise observed, however, for ejectors with 6-inch diffusers are from ½ inch to 2½ inches of water greater than those obtained with the straight ejectors of similar area and over-all length and for the same range of M_a/M_e. For the ejectors with 12-inch diffusers, the values of pressure rise are from ½ inch to 3½ inches of water greater than those for corresponding straight ejectors. In addition to the increased pressure rise or improved pumping performance obtained with diffusing exits, it is seen that they extend the range of ejector operation to higher values of M_a/M_e than achieved with straight ejectors.

The agreement between theoretical and experimental curves is of the same order as that existing for the straight ejectors; but, in several instances at low M_a/M_e, the observed values of pressure rise exceeded those predicted by theory. Theoretical curves for 85 percent of the actual area were found, however, to give best all-round improvement in the agreement between calculated and experimental results for all the diffuser ejectors tested.



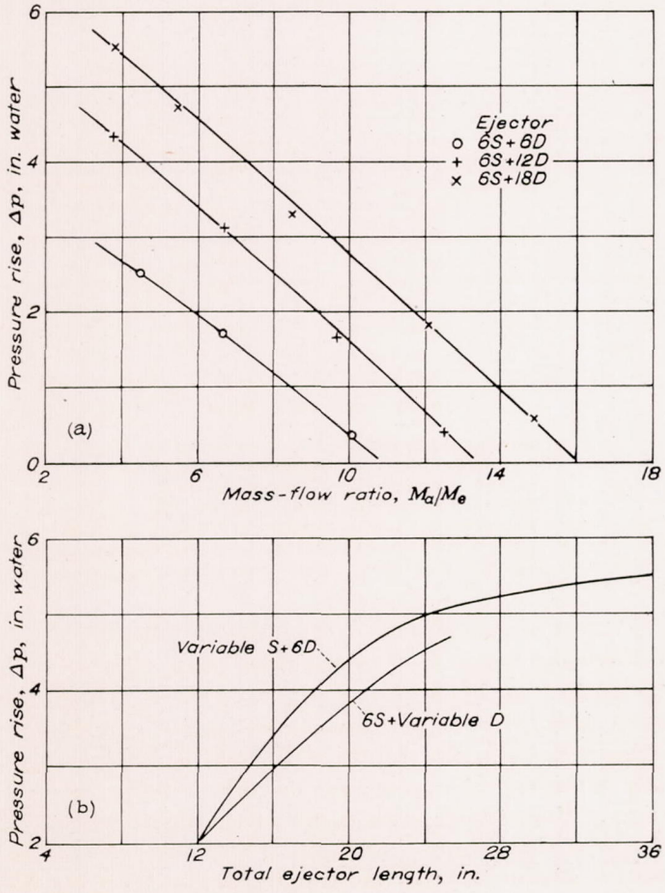
(a) Area, 20 square inches; diffuser-area ratio, 1.98.
(b) Area, 25 square inches; diffuser-area ratio, 1.87.
(c) Area, 30 square inches; diffuser-area ratio, 1.80.
(d) Area, 50 square inches; diffuser-area ratio, 1.62.

FIGURE 8.—Performance curves for 12-inch diffuser ejectors actuated by exhaust of single-cylinder engine. Aspect ratio, 3; exhaust-gas mass-flow rate, 8 pounds per minute; exhaust-nozzle area, 2.6 square inches; fuel-air ratio, 0.08; indicated horsepower, 85. For further details see table I.

The effect of length of straight section on the performance of diffuser ejectors is seen from figures 7 and 8 to be of the same nature as noted for straight ejectors. Of further interest is the relative performance of various combinations of diffuser and straight section of different length. In figure 9 (a), curves of 25-square-inch ejectors with 6-, 12-, and 18-inch diffusers and with a 6-inch straight section are plotted for comparison. In figure 9 (b), these results and those for various lengths of straight section with a 6-inch diffusing exit from figure 7 (b) are cross-plotted against over-all ejector length for an M_a/M_e of 6. All the diffuser sections were constructed with the same divergence angle; hence, the longer-length diffusers correspondingly incorporate greater expansion ratios. The improved performance of the

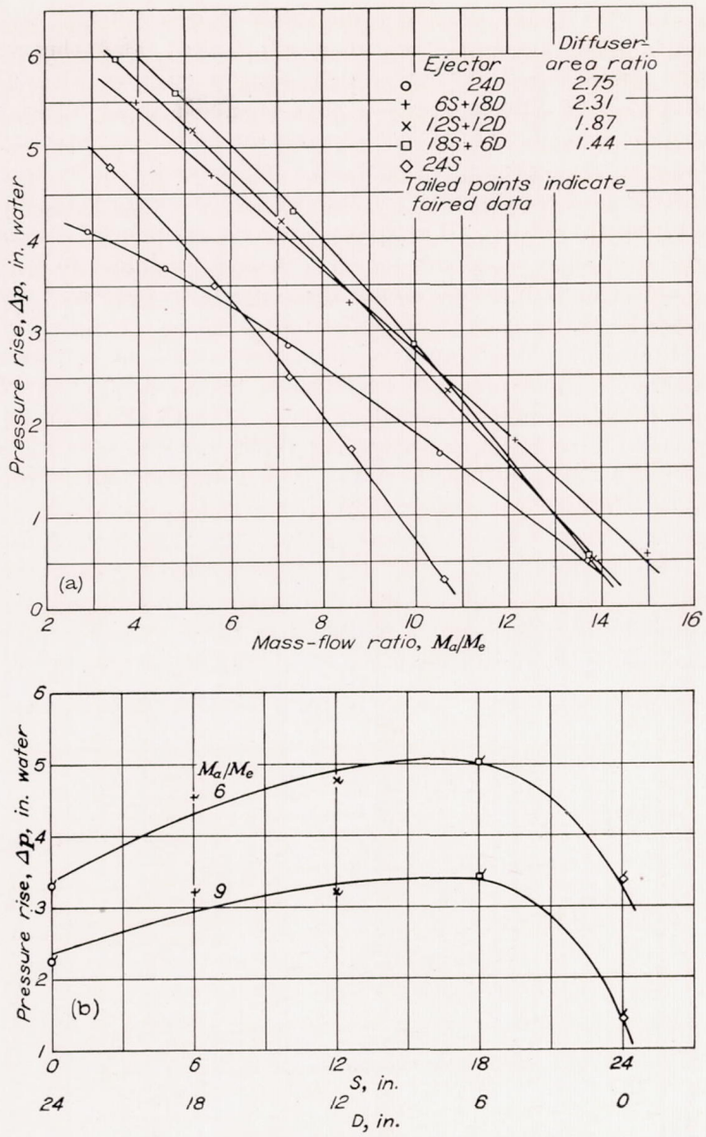
straight sections of longer length with the 6-inch diffuser over that of the straight section 6 inches in length with larger diffusers indicates the advantage of adequately long straight mixing sections. The importance of this consideration is further emphasized in figure 10 where the performance curves of various combinations of ejectors of 24-inch over-all length and 25-square-inch area are grouped (fig. 10 (a)) and are plotted against respective lengths of component straight and diffuser sections for values of M_a/M_e of 6 and 9 (fig. 10 (b)). The most advantageous utilization of the 24-inch over-all length is realized with a combination of a straight section of about 16-inch length and a diffuser of about 8-inch length. This combination is not critical, however, and has little advantage over 24-inch-length ejectors composed of 6- to 18-inch straight sections and 18- to 6-inch diffusers. The combination of longest straight section and shortest diffuser that will not impair performance is desirable from considerations of exit area.

With the long ejectors of the same over-all length the larger-expansion-ratio diffusers are advantageous; for example, the pressure rise observed for an M_a/M_e of 6 with the 24S+12D ejector was 6.0 inches of water (fig. 8 (b)) as compared with a pressure rise of 5.4 inches of water for the 30S+6D ejector (fig. 7 (b)).



(a) Performance curves.
(b) Variable straight and diffuser lengths; mass-flow ratio, 6.

FIGURE 9.—Effect of incremental straight and diffuser length on performance of ejectors actuated by exhaust of single-cylinder engine. Area, 25 square inches; ejector aspect ratio, 3; exhaust-gas mass-flow rate, 8 pounds per minute; exhaust-nozzle area, 2.6 square inches; exhaust-nozzle-exit aspect ratio, 12; fuel-air ratio, 0.08; indicated horsepower, 85. For further details see table I.



(a) Performance curves.
(b) Optimum ejector combination.

FIGURE 10.—Optimum combination of straight and diffuser sections for 24-inch over-all-length ejector. Area, 25 square inches; aspect ratio, 3; exhaust-gas mass-flow rate, 8 pounds per minute; exhaust-nozzle area, 2.6 square inches; fuel-air ratio, 0.08; indicated horsepower, 85. For further details see table I.

Various aircraft manufacturers have proposed augmenting engine cooling by the use of extremely short ejectors consisting of no more than individual exhaust stacks ejecting into the space between the cowl flaps and engine nacelle. Furthermore, results of unpublished tests comparing such installations with conventional installations of exhaust-collector rings are cited by them wherein the pseudoejector arrangement appreciably improved engine cooling.

In this connection it is interesting to note that short ejectors are relatively ineffectual in pumping action; for example, a 6S+6D ejector of 25-square-inch area provides a pressure rise of about 2.0 inches of water at an M_a/M_e of 6. Part of the improvement in engine cooling that resulted from change-over of collector-ring to individual-stack arrangement may have been due to the concomitant cleaning up of the space behind the engine in addition to ejector action.

As previously discussed, the reduced-area concept improves the agreement between experiment and theory. The performance of the straight-section ejectors with 6- and 12-inch diffusing exits is cross-plotted against mixing-section area for M_a/M_e of 6 and 9 in figures 11 and 12. Only the 85-percent-reduced-area theoretical curves are included for comparison; the full-area theoretical curves are omitted for clarity. The trends of the experimental curves and their agreement with theory is seen to be similar to that of the straight ejectors; a large discrepancy still exists at the small areas.

In order to obtain an over-all comparison of the performance of straight and diffuser ejectors, figures 6, 11, and 12 are combined and replotted in figure 13 with exit area instead of mixing-section area as the abscissa. The advantage of the 12-inch diffuser over the 6-inch diffuser and of the 6-inch diffuser over the straight ejector as regards maximum performance is clearly demonstrated; the tendency of the curves to cross at the small areas may, however, reverse the relative performance. It is also recalled, from previous discussion, that the benefits of the large diffusers will not be realized without sufficient length of mixing section.

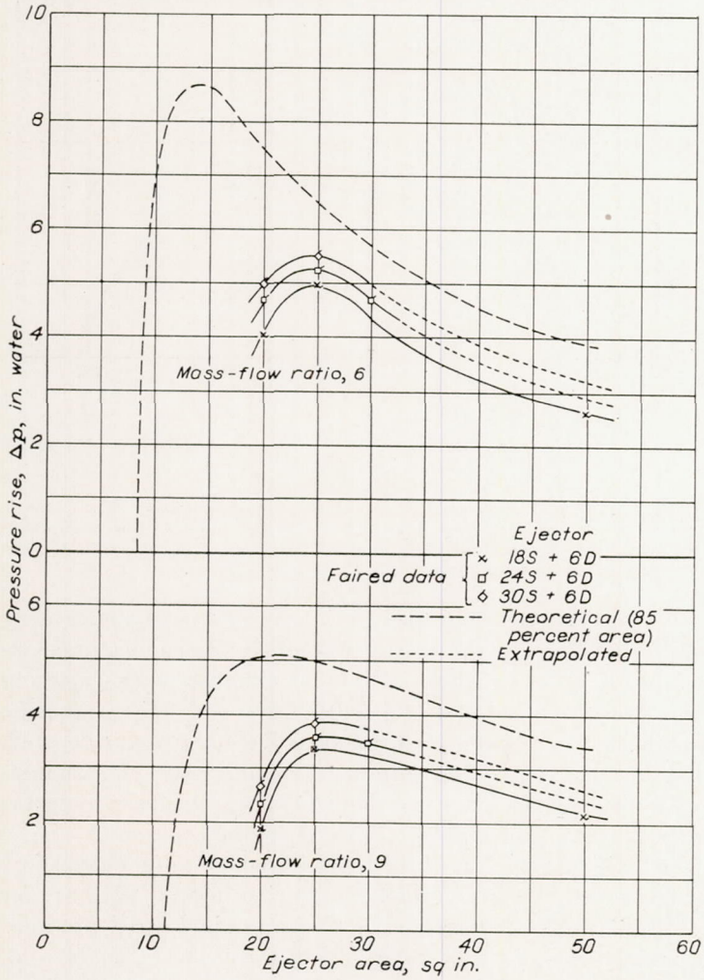


FIGURE 11.—Variation of pressure rise with ejector area for 6-inch diffuser ejectors actuated by exhaust of single-cylinder engine. Aspect ratio, 3; exhaust-gas mass-flow rate, 8 pounds per minute; exhaust-nozzle area, 2.6 square inches; fuel-air ratio, 0.08; indicated horsepower, 85.

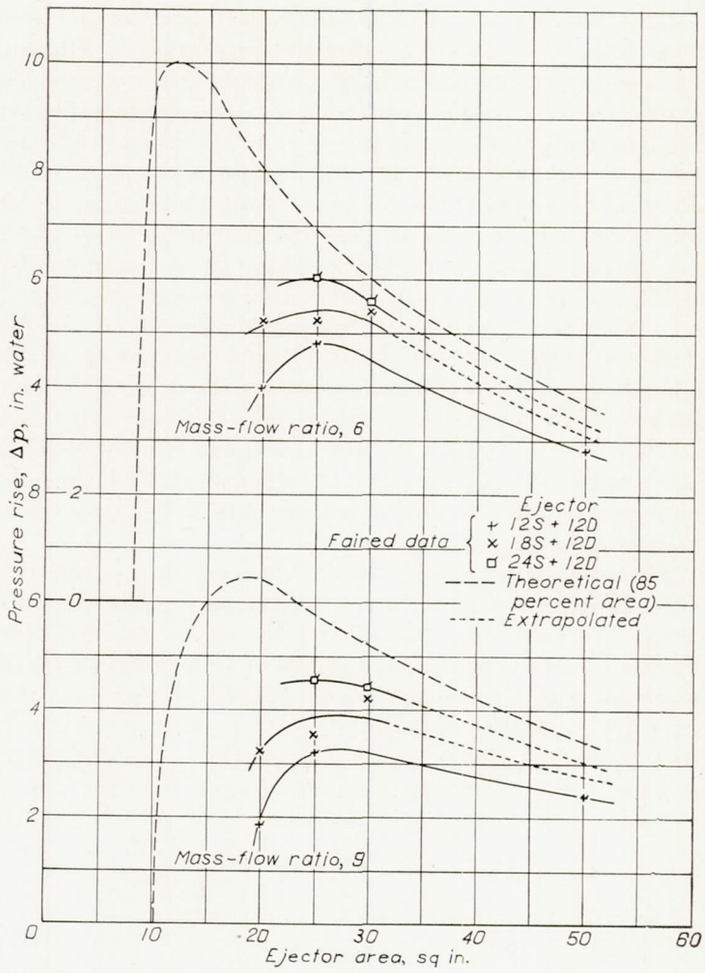


FIGURE 12.—Variation of pressure rise with ejector area for 12-inch diffuser ejectors actuated by exhaust of single-cylinder engine. Aspect ratio, 3; exhaust-gas mass-flow rate, 8 pounds per minute; exhaust-nozzle area, 2.6 square inches; fuel-air ratio, 0.08; indicated horsepower, 85.

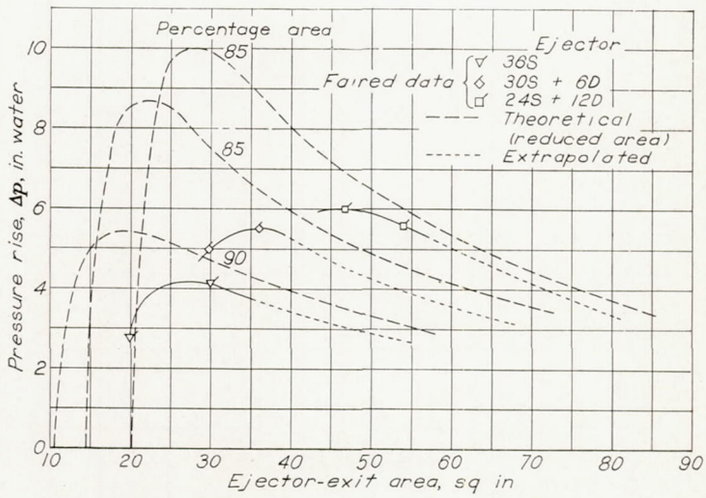


FIGURE 13.—Variation of pressure rise with ejector-exit area for straight and diffuser ejectors actuated by exhaust of single-cylinder engine. Mass-flow ratio, 6; exhaust-gas mass-flow rate, 8 pounds per minute; exhaust-nozzle area, 2.6 square inches; fuel-air ratio, 0.08; indicated horsepower, 85.

Curved ejectors.—The effect of bends in the mixing section of an ejector of 30-square-inch area with 12-inch diffusing exit is shown in figure 14, where performance curves are presented for a 30-inch straight mixing length, a 36-inch mixing length (which included a 6-in.-length 15° bend), and a 42-inch mixing length (which included two 6-in.-length reverse 15° bends). The details of these curved ejectors are shown in table II. No significant variation in performance among the arrangements is apparent. It thus appears that slight curvatures in the ejector mixing section have little, if any, unfavorable effects upon performance.

Ejector aspect ratio.—Although the investigation of ejector aspect ratio was not complete, the results of the few tests made on this phase of the problem are presented. In figure 15 the effect of aspect ratio is obtained by comparison of the performance of the 30-square-inch ejectors of 3 and 5 aspect ratio and of the 25-square-inch ejectors of 1 and 3 aspect ratio.

The performance of ejectors of aspect ratio 3 appears to be slightly better than those of aspect ratio 5 for the same nozzle of exit-area aspect ratio of 15.8. Although an ejector of aspect ratio 3 was observed to be better than an ejector of aspect ratio 1, part of the improved performance may be attributed to the fact that different exhaust nozzles were used with the 25-square-inch ejectors undergoing comparison. The square exhaust nozzle used with the ejector of aspect ratio 1 is not, as will be discussed later, as effective as a flat nozzle of the type used with the ejector of aspect ratio 3. It is considered, therefore, that the actual advantage of aspect ratio 3 is slight.

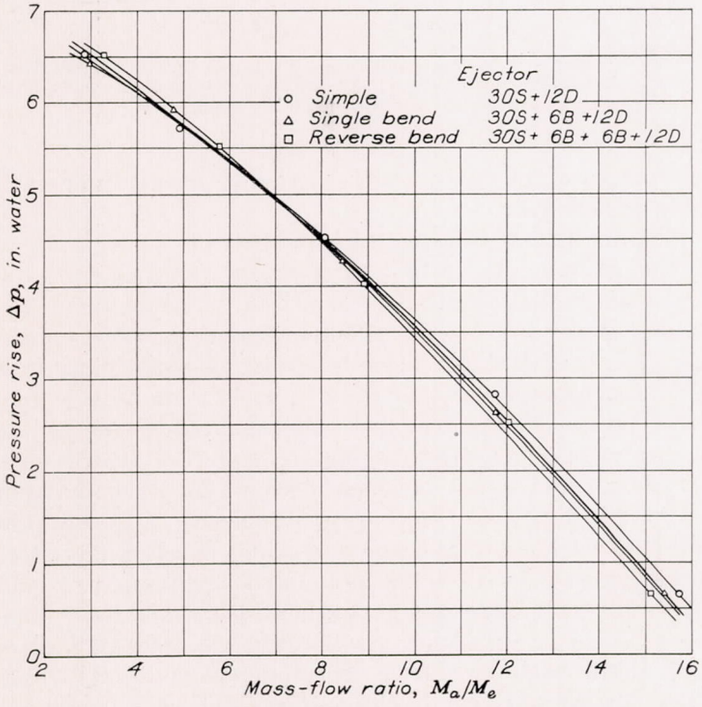


FIGURE 14.—Performance curves for curved ejectors actuated by exhaust of single-cylinder engine. Area, 30 square inches; aspect ratio, 3; exhaust-gas mass-flow rate, 8 pounds per minute; exhaust-nozzle area, 2.6 square inches; fuel-air ratio, 0.08; indicated horsepower, 85. For further details see table II.

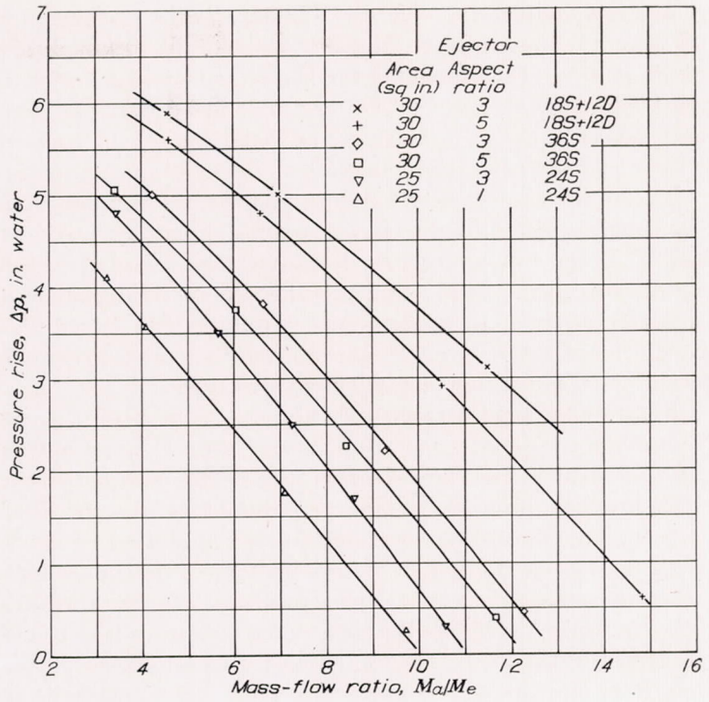


FIGURE 15.—Effect of mixing-section aspect ratio on performance of ejectors actuated by exhaust of single-cylinder engine. Exhaust-gas mass-flow rate, 8 pounds per minute; exhaust-nozzle area, 2.6 square inches; fuel-air ratio, 0.08; indicated horsepower, 85. For further details see table I.

The effect of aspect ratio on ejector action may be considered in terms of length—hydraulic-diameter ratio because, for constant area, change in aspect ratio changes the hydraulic diameter and therefore, for a given length, changes the L/D_h. Thus the small improvement in performance obtained by increasing the aspect ratio from 1 to 3 may be thought of as being due to increased mixing efficiency resulting from increase in L/D_h and the subsequent slight depreciation in performance with further increase of aspect ratio as being the result of increased friction effects' overcompensating the benefits of improved mixing.

Divided ejectors.—The tests of the divided ejectors (see table II) were an extension of the investigation of ejector aspect ratio and were prompted by the idea that improved performance of short-length ejectors could be obtained by decreasing the hydraulic diameter and consequently increasing the L/D_h. In figure 16 the results of the divided 25-square-inch ejector are compared with those of the simple or undivided ejectors of 25-square-inch area and aspect ratio of 3. Despite the 25-percent-smaller hydraulic diameter and the greater L/D_h of the divided ejectors, their performance was poorer than that of the undivided ejectors. The depreciation in performance may have been caused by additional losses incurred in the branched exhaust nozzle and by increased friction effects.

Multistage ejectors.—Figure 17 illustrates the performance of the multistage ejector, the physical details of which are given in table II. Included for comparison is the performance curve of the 24S+12D ejector of 30-square-inch area and aspect ratio of 3, the over-all length and exit area of which corresponds closely to that of the multistage ejector.

The multistage ejector exhibits poorer performance than the single-stage diffuser ejector over a great part of the M_a/M_e range but appears to be slightly better at the high end of the range. It thus appears that the multistage ejector is better adapted to applications requiring high flows; this conclusion cannot, however, be considered general inasmuch as only one multistage arrangement was tested.

Nozzle-exit aspect ratio.—During the course of the investigation, exhaust nozzles of various aspect ratios and of 2.6-square-inch exit area were tested with several of the different-area ejectors. Some representative results illustrating the effect of nozzle aspect ratio are plotted in figure 18 (a). The performance of the ejectors of 25-square-inch area and aspect ratio of 1 with nozzles of aspect ratio of 7 ($4\frac{9}{32}$ by $3\frac{9}{64}$ in.) is better than the same ejectors with nozzles of aspect ratio of 1 ($1\frac{5}{8}$ by $1\frac{5}{8}$ in.). Comparison of the results of ejectors of 30-square-inch area and aspect ratio of 5 shows the 15.8-aspect-ratio nozzle ($6\frac{13}{32}$ by $\frac{13}{32}$ in.) to be better than the 41.7-aspect-ratio nozzle ($10\frac{13}{32}$ by $\frac{1}{4}$ in.) and the performance of the ejectors of 30-square-inch area and aspect ratio of 3 indicates a slight advantage of the 15.8-aspect-ratio nozzle over that of the 12.0-aspect-ratio nozzle ($5\frac{19}{32}$ by $\frac{19}{32}$ in.). It thus appears that flattening out the exhaust nozzle to a certain extent provides improved ejector performance but that excessive flattening results in depreciated performance.

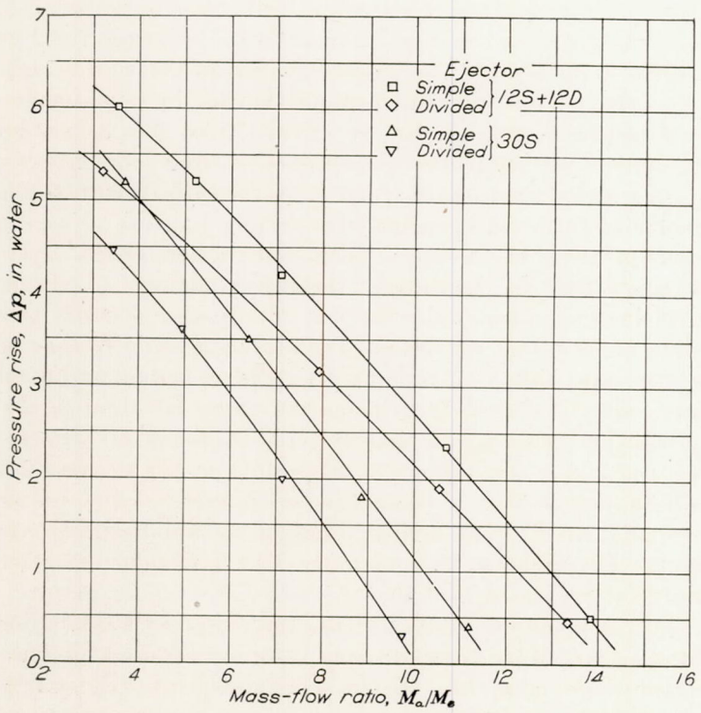


FIGURE 16.—Performance curves for divided ejectors actuated by exhaust of single-cylinder engine. Area, 25 square inches; aspect ratio, 3; exhaust-gas mass-flow rate, 8 pounds per minute; exhaust-nozzle area, 2.6 square inches; fuel-air ratio, 0.08; indicated horsepower, 85. For further details see table II.

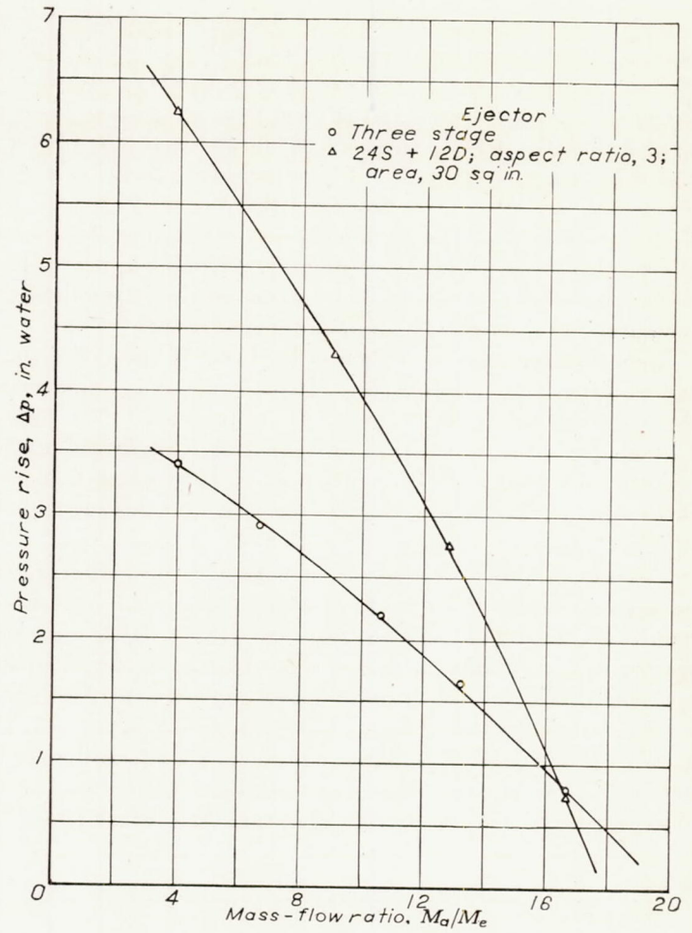
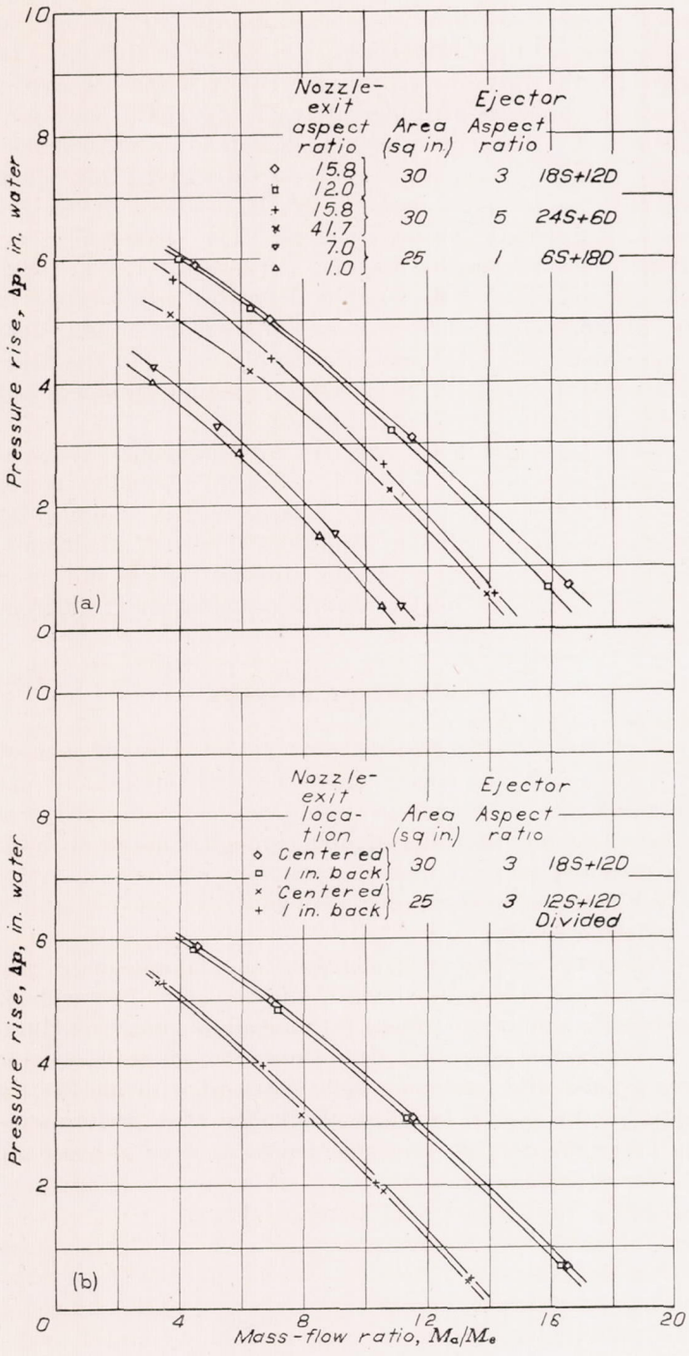


FIGURE 17.—Performance curves for multistage ejector actuated by exhaust of single-cylinder engine. Exhaust-gas mass-flow rate, 8 pounds per minute; exhaust-nozzle area, 2.6 square inches; fuel-air ratio, 0.08; indicated horsepower, 85. For further details see table II.

The improved performance with the wide exhaust nozzle is undoubtedly due to the better mixing resulting from the increased surface area of the exhaust jet. The reason for the falling off in performance with the extremely wide nozzle is not readily apparent. There is a very good possibility that the cross-sectional area of the extremely wide nozzles may have appreciably increased during operation owing to the action of the high-pressure, high-temperature exhaust gas. The larger area would, of course, decrease the jet momentum and hence decrease the ejector performance. Although precautions in the form of reinforcing bands and through-rivets were taken to avoid enlargement, only a slight bulging would cause a large increase in area for the wide flat nozzles. Inasmuch as the practicability of extremely wide exhaust nozzles was questionable because of their inherent structural weakness, further tests with additional precautions to maintain the desired cross-sectional area with these nozzles were not conducted.

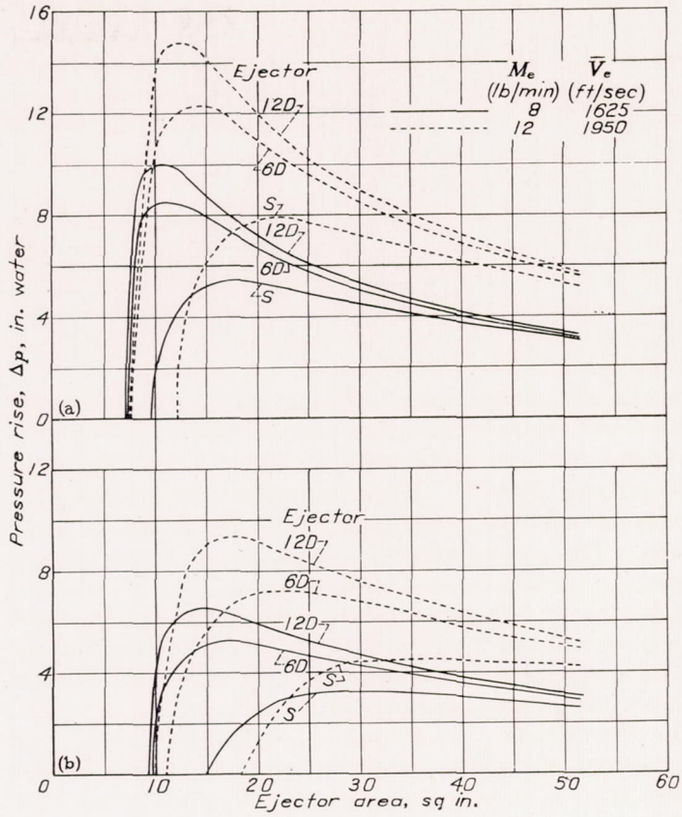
It is believed that, in general, increase in surface area of the primary jet will improve the performance of ejectors provided that the jet momentum is not reduced.

Nozzle-exit location.—A few tests were made with the exhaust-nozzle exit located 1 inch upstream of the center of the ejector-entrance section. The results of these tests are compared in figure 18 (b) with the results obtained with the nozzle in the central position. No significant difference in performance is indicated.



(a) Nozzle-exit aspect ratio.
(b) Nozzle-exit location.

FIGURE 18.—Effect of nozzle-exit aspect ratio and nozzle-exit location on performance of ejectors actuated by exhaust of single-cylinder engine. Exhaust-gas mass-flow rate, 8 pounds per minute; exhaust-nozzle area, 2.6 square inches; fuel-air ratio, 0.08; indicated horsepower, 85.



(a) Mass-flow ratio, 6.
(b) Mass-flow ratio, 9.

FIGURE 19.—Theoretical variation of pressure rise with ejector area for straight and diffuser ejectors for two exhaust-gas mass-flow rates. Exhaust-gas temperature, 1500° F; air temperature, 75° F; exhaust-nozzle area, 2.6 square inches.

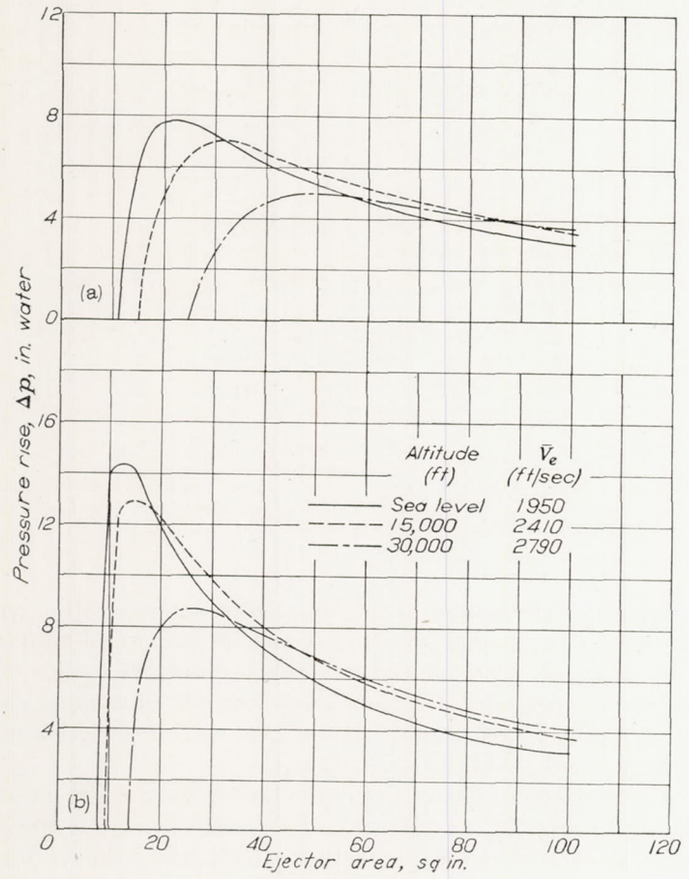
Ejector performance at higher engine power.—Although the maximum engine power at which experimental results were obtained was limited to cruise value (85 indicated horsepower corresponding to a mass-flow rate of exhaust gas M_e of 8 pounds per minute), theoretical ejector performance at high power should be considered.

For purposes of illustration, calculations were made for an M_e of 12 pounds per minute, which corresponds to about rated power. The mean effective exhaust-gas velocity was taken at 1950 feet per second as obtained from reference 4 for the same exhaust-nozzle area as used in the tests (2.6 sq in.). The results of the calculations are shown in figure 19 (a) where pressure rise is plotted against ejector area for an M_a/M_e of 6 for cases of straight, 6-inch diffuser, and 12-inch diffuser ejectors. The previously considered theoretical curves for an M_e of 8 pounds per minute are included for comparison. Similar sets of curves are presented in figure 19 (b) for an M_a/M_e of 9.

The curves for an M_e of 12 pounds per minute are similar to those for an M_e of 8 pounds per minute except for higher values of pressure rise. If the large difference in pressure rise occurring at the small areas is neglected, an increase in pressure rise from 2 to 3½ inches of water is indicated for the

high-power condition for an M_a/M_e of 6 and an increase in pressure rise from 2 to 3 inches of water for an M_a/M_e of 9. It is noted that the performance curves for an M_e of 12 pounds per minute peak at larger area than do the curves for an M_e of 8 pounds per minute.

It is appreciated that the peak values of pressure rise indicated by theory will be as unattainable in practice for an M_e of 12 pounds per minute as they were observed to be for an M_e of 8 pounds per minute. It is reasonable to assume, however, that the actual difference in performance between operation at an M_e of 12 pounds per minute and an M_e of 8 pounds per minute will closely approximate the theoretical differences previously noted. These values will probably be somewhat decreased owing to the large friction at the higher power. In addition, it is expected that the actual areas yielding optimum performance will be larger than corresponding areas for the low-power condition.



(a) Straight ejector.
(b) 12-inch diffuser ejector.

FIGURE 20.—Theoretical variation of pressure rise with ejector area at various altitudes. Mass-flow ratio, 6; exhaust-gas mass-flow rate, 12 pounds per minute; exhaust-gas temperature, 1500° F; air temperature, 75° F; exhaust-nozzle area, 2.6 square inches.

Altitude performance.—The performance of ejectors at altitude is of interest. In lieu of experimental results, theoretical values have been considered in order to indicate the trends of ejector performance with variation in altitude. In figure 20, the variation of pressure rise with ejector area is shown for pressure altitudes at sea level, 15,000 feet, and 30,000 feet. The curves were calculated for an exhaust-nozzle area of 2.6 square inches, an exhaust-gas mass-flow rate of 12 pounds per minute, an M_a/M_e of 6, and for straight and 12-inch-length diffuser ejectors. The ejector air temperature was arbitrarily assumed constant at 75° F. The peak pressure rise of the ejectors decreases with increase in altitude and occurs at larger values of area; the second effect is more marked for the nondiffusing ejectors. In the practical range beyond the peak values, altitude produces but slight change in ejector performance.

Use of the nozzle of exit area of 2.6 square inches, designed for zero power loss at sea level, will incur an engine power loss with increase in altitude. A larger nozzle, designed for zero power loss at particular conditions of power and altitude, will not produce as large ejector pressure rises as indicated in figure 20, but the relative ejector performance at different altitudes will be similar.

SUMMARY OF RESULTS

From tests of rectangular ejectors, actuated by the exhaust of a single-cylinder engine operating with an exhaust-gas mass-flow rate of 8 pounds per minute corresponding to cruise power of 85 indicated horsepower through a nozzle with an exit area of 2.6 square inches, it was found that:

1. Ejector pressure rise increased with decrease in quantity of air pumped.

2. Ejector performance increased at a diminishing rate with increase in length. Lengths of about 6 or 7 diameters, although not optimum, constituted adequate practical values.

3. For given operating conditions, an optimum ejector area existed, the value of which increased with increase in mass-flow ratio. At the test conditions, best performance with straight ejectors was indicated at an area of about 27

square inches for a mass-flow ratio of 6 and at an area of about 30 square inches for a mass-flow ratio of 9; for an ejector 30 inches in length, the pressure rises were 3.8 inches of water and 2.0 inches of water, respectively.

4. Diffuser-exit sections considerably improved the performance of the ejectors; the use of a diffuser of 12-inch length and 1.87 area ratio attached to a straight section of 24-inch length and 25-square-inch area resulted in a pressure rise of 6 inches of water for a mass flow of air representative of cooling requirements (six times the mass flow of engine exhaust gas). Although this gain was obtained at the expense of increased exit area, the performance of diffuser ejectors was also better than that of straight ejectors for the same exit area and over-all length.

5. Ejector cross-sectional aspect ratio had small effect; with the exhaust-gas nozzles used, ejectors of aspect ratio of 3 gave slightly improved performance over those with aspect ratios of 1 and 5.

6. The performance of divided ejectors formed by insertion of an axial separating plate in a 25-square-inch ejector actuated by flow from a forked exhaust-gas nozzle was poorer than the performance of the original undivided ejector.

7. A three-stage ejector exhibited poorer pumping characteristics than a single-stage diffuser ejector of the same over-all length and exit area.

8. The inclusion of 15° single and reverse bends in the mixing section of an ejector did not noticeably impair its performance.

9. Flattened exhaust-gas nozzles with cross-sectional aspect ratios of approximately 12 to 15 provided better ejector performance than nozzles of either smaller or larger aspect ratios.

10. Simple steady-flow ejector theory predicted performance of straight and diffuser ejectors in fair agreement with experimental results over the range of ejector configuration tested; peak values of pressure rise predicted at small ejector areas were unattainable. Optimum ejector-area values prescribed by theory were smaller than indicated by test.

AIRCRAFT ENGINE RESEARCH LABORATORY,
NATIONAL ADVISORY COMMITTEE FOR AERONAUTICS,
CLEVELAND, OHIO, *May 1, 1944.*

APPENDIX

DERIVATION OF EQUATIONS

SYMBOLS

A ejector cross-sectional area, sq ft

A_e cross-sectional area of exhaust-gas jet at section 1, sq ft

c_p specific heat at constant pressure, Btu/(slug) (°F)

D_h hydraulic diameter of ejector cross section $\left(\frac{4A}{\text{perimeter}}\right)$, in.

k_d loss coefficient in diffuser

L straight-mixing-section length of ejector, in.

M average mass rate of gas flow, slugs/sec

p static pressure, lb/sq ft

Δp pressure rise, lb/sq ft or in. water

R gas constant, ft-lb/(slug) (°F)

T gas temperature, °R

V average gas velocity, ft/sec

$\overline{V}$ mean effective gas velocity, ft/sec

α factor accounting for reduction of ejector-entrance area due to presence of exhaust-gas jet $\left[\frac{A_2(A_2-2A_e)}{(A_2-A_e)^2}\right]$

β diffuser factor $\left[1-\left(\frac{A_2}{A_3}\right)^2-k_d\left(1-\frac{A_2}{A_3}\right)^2\right]$

ρ density of gas, slugs/cu ft

Subscripts:

a with reference to cooling air

e with reference to exhaust gas

m with reference to mixture

0 entrance to convergent section of ejector

1 entrance to straight mixing section

2 exit of straight mixing section or entrance to diffuser

3 exit of diffusing section

SIMPLIFIED ANALYSIS

The basic principles of the ejector pump are elementary; a rigorous analysis of the processes involved is, however, extremely complicated. Although existing analyses incorporate, of necessity, simplifying assumptions, the final equations are rather unwieldy and not in a form readily applicable to an investigation of ejectors actuated by the exhaust gas of an aircraft engine.

The simplified analysis that follows considers the effect of pertinent variables and predicts performance in terms of known engine quantities. The pressure rise across the ejector is obtained as a function of the mass-flow rate of air pumped, the ejector cross-sectional area, and the mass-flow rate and velocity of exhaust gas available.

The effect of the pulsating exhaust gas is taken into account by the use of an effective exhaust-gas velocity $\overline{V}_e$ introduced in reference 4 as that equivalent velocity which, when multiplied by the steady-flow average mass-flow rate of exhaust gas, would produce the average momentum obtained by thrust measurements. In view of the complicated nature of the pulsating air and the mixture flow and their dependence upon M_a/M_e, ejector dimensions, and engine operating conditions, steady-flow values are assumed.

Straight ejectors.— A uniform velocity distribution and complete mixing are assumed at station 2. (See fig. 3.) If the laws of conservation of momentum and conservation of mass are applied between stations 1 and 2 and if friction is neglected, the following equation may be written

$$M_e\overline{V}_e+M_aV_{a,1}+p_1A_1=(M_a+M_e)\ V_{m,2}+p_2A_2 \tag{1}$$

If the equation is rearranged and the pressure rise across the mixing section wherein $A_1=A_2$ is solved

$$p_2-p_1=\frac{M_e\overline{V}_e}{A_2}+\frac{M_aV_{a,1}}{A_2}-\frac{(M_a+M_e)V_{m,2}}{A_2} \tag{2}$$

The air and mixture velocities may be expressed as

$$V_{m,2}=\frac{(M_a+M_e)}{\rho_{m,2}A_2} \tag{3}$$

and

$$V_{a,1}=\frac{M_a}{\rho_{a,1}(A_2-A_e)}$$

where A_e is the cross-sectional area of the exhaust-gas jet at station 1. The pressure differences existing throughout the ejector in the present application have negligible effect upon density; hence $\rho_{a,1}$ may be taken as equal to $\rho_{a,0}$, or simply as ρ_a, and in conjunction with the perfect-gas equation

$$\rho_{m,2}=\rho_m=\frac{\rho_aR_aT_a}{R_mT_m} \tag{4}$$

When equations (3) and (4) are substituted in equation (2), there is obtained

$$p_2-p_1=\frac{M_e\overline{V}_e}{A_2}+\frac{M_a^2}{\rho_a A_2(A_2-A_e)}-\frac{(M_a+M_e)^2}{A_2^2\rho_a}\frac{R_mT_m}{R_aT_a} \tag{5}$$

If Bernoulli's equation is applied between stations 0 and 1 and the air velocity at station 0 is assumed to be equal to zero,

$$p_1=p_0-\frac{1}{2}\rho_a V_{a,1}^2$$

or

$$p_1-p_0=-\frac{1}{2}\frac{M_a^2}{\rho_a(A_2-A_e)^2} \tag{6}$$

The pressure rise from 0 to 2 is obtained from equations (5) and (6)

$$p_2-p_0=\frac{M_e\overline{V}_e}{A_2}+\frac{M_a^2}{\rho_a A_2(A_2-A_e)}-\frac{1}{2}\frac{M_a^2}{\rho_a(A_2-A_e)^2}-\frac{(M_a+M_e)^2}{A_2^2\rho_a}\frac{R_mT_m}{R_aT_a} \tag{7}$$

which may be written

$$p_2-p_0=\frac{M_e\overline{V}_e}{A_2}+\left(\frac{M_e}{A_2}\right)^2\frac{1}{\rho_a}\frac{M_a}{M_e}\left[\frac{\alpha}{2}\frac{M_a}{M_e}-\left(\frac{M_a}{M_e}+1\right)\left(\frac{M_e}{M_a}+1\right)\frac{R_mT_m}{R_aT_a}\right] \tag{8}$$

where

$$\alpha=\frac{A_2(A_2-2A_e)}{(A_2-A_e)^2}$$

is the factor accounting for the reduction in available area for air flow in station 1 due to the presence of the exhaust-gas jet. For practical cases A_e is small relative to A_2 and α may be taken as unity.

R_m and T_m may be expressed in terms of the properties and temperatures of the air and the exhaust gas.

From the general energy equation, neglecting the kinetic-energy terms, there is obtained

$$(M_a+M_e)c_{p,m}T_m=M_ac_{p,a}T_a+M_ec_{p,e}T_e \tag{9}$$

The specific heat of the gas mixture is given by

$$c_{p,m}=\frac{(M_a/M_e)c_{p,a}+c_{p,e}}{(M_a/M_e)+1} \tag{10}$$

Similarly, the gas constant of the gas mixture is given by

$$R_m=\frac{(M_a/M_e)R_a+R_e}{(M_a/M_e)+1} \tag{11}$$

Equations (9), (10), and (11) are combined to obtain

$$\frac{R_mT_m}{R_aT_a}=\frac{\left(\frac{M_a}{M_e}+\frac{R_e}{R_a}\right)\left(\frac{M_a}{M_e}+\frac{c_{p,e}}{c_{p,a}}\frac{T_e}{T_a}\right)}{\left(\frac{M_a}{M_e}+1\right)\left(\frac{M_a}{M_e}+\frac{c_{p,e}}{c_{p,a}}\right)} \tag{12}$$

By substitution of equation (12) in equation (8)

$$p_2-p_0=\frac{M_e\overline{V}_e}{A_2}+\left(\frac{M_e}{A_2}\right)^2\frac{1}{\rho_a}\frac{M_a}{M_e}\left[\frac{\alpha}{2}\frac{M_a}{M_e}-\left(\frac{M_e}{M_a}+1\right)\left(\frac{M_a}{M_e}+\frac{R_e}{R_a}\right)\frac{\left(\frac{M_a}{M_e}+\frac{c_{p,e}}{c_{p,a}}\frac{T_e}{T_a}\right)}{\left(\frac{M_a}{M_e}+\frac{c_{p,e}}{c_{p,a}}\right)}\right] \tag{13}$$

If the difference in specific heats and gas constants between air and exhaust gas is neglected and if the area of the exhaust-gas jet is small compared with the area of the ejector, equation (13) may be simplified to

$$p_2-p_0=\frac{M_e\overline{V}_e}{A_2}+\left(\frac{M_e}{A_2}\right)^2\frac{1}{\rho_a}\frac{M_a}{M_e}\left[\frac{1}{2}\frac{M_a}{M_e}-\left(\frac{M_a}{M_e}+1\right)\left(1+\frac{M_e}{M_a}\frac{T_e}{T_a}\right)\right] \tag{14}$$

which may be written

$$p_2-p_0=\frac{M_e\overline{V}_e}{A_2}+\frac{1}{\rho_a}\left(\frac{M_e}{A_2}\right)^2 f\left(\frac{M_a}{M_e},\frac{T_e}{T_a}\right) \tag{15}$$

Thus the pressure rise of the exhaust-gas ejector pump is given as the sum of two terms: (1) the exhaust-gas thrust per unit ejector area and (2) the product of the square of the mass-flow rate of exhaust gas per unit ejector area, the specific volume of air, and a function of the mass-flow ratio and of the ratio of exhaust-gas temperature to air temperature. The second term is negative for all values of M_a/M_e.

With the range of variables encountered, the second term of the right side of equation (14) is negative indicating the existence of an optimum ejector area.

Diffusing exits.—Addition of a diffusing exit to the straight ejector permits conversion of part of the kinetic head into pressure head. The pressure rise attributable to the diffuser may be readily evaluated in terms of the pertinent factors already used. Application of Bernoulli's equation and the continuity equation between stations 2 and 3 and assumption of constant density gives the familiar diffuser equation

$$p_3-p_2=\frac{1}{2}\rho_m V_{m,2}^2\left[1-\left(\frac{A_2}{A_3}\right)^2\right] \tag{16}$$

The efficiency of pressure recovery of a diffuser is dependent upon both the expansion angle and the expansion ratio. Equation (16) is thus modified to

$$p_3-p_2=\frac{1}{2}\rho_m V_{m,2}^2\left[1-\left(\frac{A_2}{A_3}\right)^2-k_d\left(1-\frac{A_2}{A_3}\right)^2\right] \tag{17}$$

where k_d, the loss coefficient in the diffuser, is a function of diffuser angle.

Substitution of the expressions for $V_{m,2}$, ρ_m, and $\frac{R_m T_m}{R_a T_a}$ from equations (3), (4), and (12) in equation (17) gives

$$p_3-p_2=\frac{1}{2\rho_a}\left(\frac{M_a+M_e}{A_2}\right)^2\left[1-\left(\frac{A_2}{A_3}\right)^2-k_d\left(1-\frac{A_2}{A_3}\right)^2\right]\left[\frac{\left(\frac{M_a}{M_e}+\frac{R_e}{R_a}\right)\left(\frac{M_a}{M_e}+\frac{c_{p,e}}{c_{p,a}}\frac{T_e}{T_a}\right)}{\left(\frac{M_a}{M_e}+1\right)\left(\frac{M_a}{M_e}+\frac{c_{p,e}}{c_{p,a}}\right)}\right] \tag{18}$$

With addition of equation (18) to equation (13), the total pressure rise in an ejector ($p_3-p_0=\Delta p$) with a diffuser exit becomes

$$\Delta p=\frac{M_e\overline{V}_e}{A_2}+\left(\frac{M_e}{A_2}\right)^2\frac{1}{\rho_a}\frac{M_a}{M_e}\left[\frac{\alpha}{2}\frac{M_a}{M_e}+\left(\frac{M_e}{M_a}+1\right)\left(\frac{M_a}{M_e}+\frac{R_e}{R_a}\right)\frac{\left(\frac{M_a}{M_e}+\frac{c_{p,e}}{c_{p,a}}\frac{T_e}{T_a}\right)}{\left(\frac{M_a}{M_e}+\frac{c_{p,e}}{c_{p,a}}\right)}\left(\frac{\beta}{2}-1\right)\right] \tag{19}$$

where

$$\beta=\left[1-\left(\frac{A_2}{A_3}\right)^2-k_d\left(1-\frac{A_2}{A_3}\right)^2\right]$$

If the simplifying assumption made in going from equation (13) to equation (14) is again applied, equation (19) reduces to

$$\Delta p=\frac{M_e\overline{V}_e}{A_2}+\left(\frac{M_e}{A_2}\right)^2\frac{1}{\rho_a}\frac{M_a}{M_e}\left[\frac{1}{2}\frac{M_a}{M_e}+\left(\frac{M_a}{M_e}+1\right)\left(1+\frac{M_e}{M_a}\frac{T_e}{T_a}\right)\left(\frac{\beta}{2}-1\right)\right] \tag{20}$$

Equation (19) or (20) may be considered the general equation for straight as well as diffuser ejectors. For straight ejectors $\beta=0$ and equation (19) reduces to equation (13) and equation (20) reduces to equation (14). The theoretical curves used in this report were calculated by means of equation (19); over the range of ejector operation of practical interest in the present application, use of the approximate equation (20) introduces negligible deviation from equation (19). (See fig. 21.)

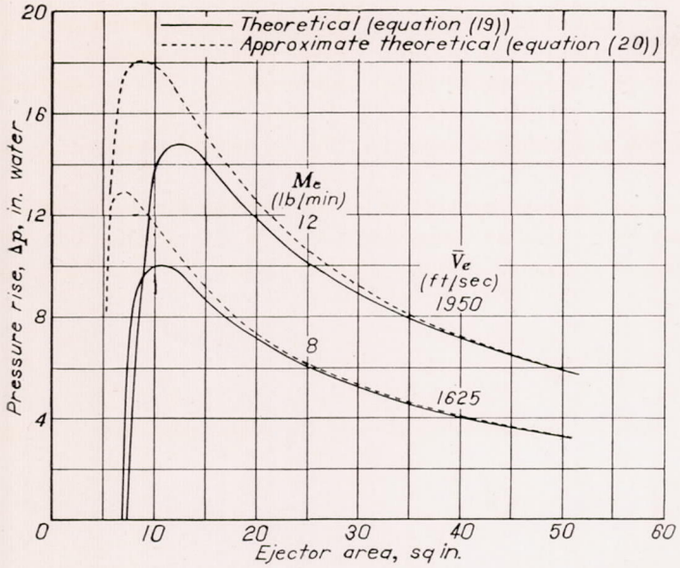
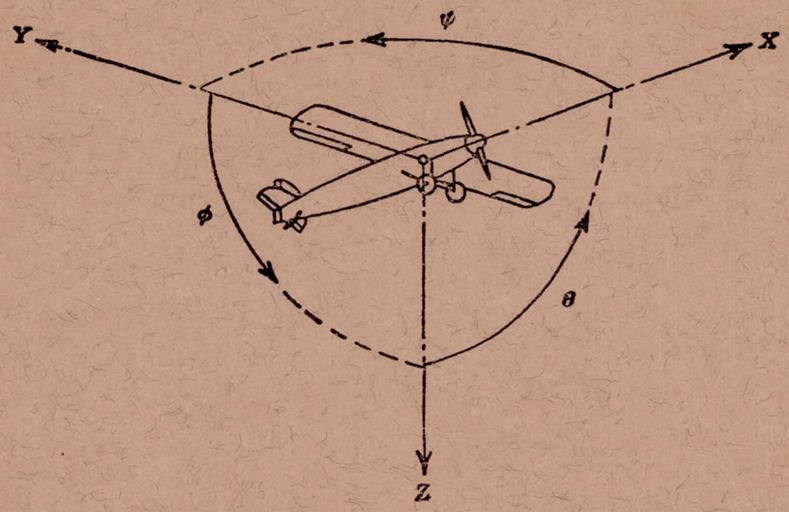


FIGURE 21.—Comparison of theoretical performance of 12-inch diffuser ejector as predicted by equation (19) and approximate equation (20). Mass-flow ratio, 6; exhaust-gas temperature, 1500° F; air temperature, 75° F; exhaust-nozzle area, 2.6 square inches.

REFERENCES

1. Jacobs, Eastman N., and Shoemaker, James M.: Tests on Thrust Augmentors for Jet Propulsion. NACA TN No. 431, 1932.
2. Schubauer, G. B.: Jet Propulsion with Special Reference to Thrust Augmentors. NACA TN No. 442, 1933.
3. Manganiello, Eugene J.: A Preliminary Investigation of Exhaust-Gas Ejectors for Ground Cooling. NACA ACR, July 1942.
4. Pinkel, Benjamin, Turner, L. Richard, and Voss, Fred: Design of Nozzles for the Individual Cylinder Exhaust Jet Propulsion System. NACA ACR, April 1941.
5. Ebaugh, N. C., and Whitfield, R.: The Intake Orifice and a Proposed Method for Testing Exhaust Fans. A.S.M.E. Trans., PTC–56–3, vol. 56, no. 12, Dec. 1934, pp. 903–911.
6. Patterson, G. N.: Modern Diffuser Design. Aircraft Engineering, vol. X, no. 115, Sept. 1938, pp. 267–273.
7. Flügel, Gustav: The Design of Jet Pumps. NACA TM No. 982, 1941.

U. S. GOVERNMENT PRINTING OFFICE: 1948



Positive directions of axes and angles (forces and moments) are shown by arrows

Axis		Force (parallel to axis) symbol	Moment about axis			Angle		Velocities	
Designation	Symbol		Designation	Symbol	Positive direction	Designation	Symbol	Linear (component along axis)	Angular
Longitudinal	X	X	Rolling	L	$Y \longrightarrow Z$	Roll	ϕ	u	p
Lateral	Y	Y	Pitching	M	$Z \longrightarrow X$	Pitch	θ	v	q
Normal	Z	Z	Yawing	N	$X \longrightarrow Y$	Yaw	ψ	w	r

Absolute coefficients of moment

$C_l = \frac{L}{qbS}$ (rolling) $\quad C_m = \frac{M}{qcS}$ (pitching) $\quad C_n = \frac{N}{qbS}$ (yawing)

Angle of set of control surface (relative to neutral position), δ. (Indicate surface by proper subscript.)

4. PROPELLER SYMBOLS

D Diameter

p Geometric pitch

p/D Pitch ratio

V' Inflow velocity

V_s Slipstream velocity

T Thrust, absolute coefficient $C_T = \frac{T}{\rho n^2 D^4}$

Q Torque, absolute coefficient $C_Q = \frac{Q}{\rho n^2 D^5}$

P Power, absolute coefficient $C_P = \frac{P}{\rho n^3 D^5}$

C_s Speed-power coefficient $= \sqrt[5]{\frac{\rho V^5}{P n^2}}$

η Efficiency

n Revolutions per second, rps

Φ Effective helix angle $= \tan^{-1}\left(\frac{V}{2\pi r n}\right)$

5. NUMERICAL RELATIONS

1 hp=76.04 kg-m/s=550 ft-lb/sec

1 metric horsepower=0.9863 hp

1 mph=0.4470 mps

1 mps=2.2369 mph

1 lb=0.4536 kg

1 kg=2.2046 lb

1 mi=1,609.35 m=5,280 ft

1 m=3.2808 ft